QED FSR for the ϕ^*_η observable and its systematic errors

Z. Was*

*Institute of Nuclear Physics, Krakow

Lepton directions: *are precisely measured at LHC experiments, better by the order of magitude than any other quantity*

1. *It is very attractive to explore this quantity.*
2. *One of the obervables aiming at this purpose is ϕ^*_η of the previous talk.*
3. *Measurements/reconstruction of lepton (directions) can not be separated from final state bremsstrahlung*

How to use lepton directions *in as universal and hard process independent way as possible*

1. What is the precision of QED FSR for LHC applications?
2. Is QED FSR a separate phenomenological unit or it must be considered as inseparable part of electroweak + hadronic interactions as well?

Introduction

My talk is based on two papers of the last winter:

- T. K. O. Doan, W. Placzek and Z. Was, "Observable ϕ^*_η at LHC and second-order QED matrix element in $Z/\gamma \to l^+l^-$ decays," arXiv:1303.2220
- A. B. Arbuzov, R. R. Sadykov and Z. Was, "QED Bremsstrahlung in decays of electroweak bosons," arXiv:1212.6783

But also, and may be first of all on discussion and questions from my experimental colleagues: Ashutosh Kotwal, Thi Kieu Oanh Doan, Lucia di Ciaccio, Maarten Boonekamp, Jan Kretzschmar, Daniel Frodevaux and many others:

- What is the syst. error for results of MC progams simulating FSR in Z or W decays?
- What is the systematic error for separation of QED FSR from the rest of Electroweak/hadronic interaction.
- What is an overall systematic error for ϕ^*_η observable?

Question may arise: What work was behind comparison of results for QED simulation from PHOTOS and SHERPA for ϕ^*_η observable.

Comparison plots taken from experiments

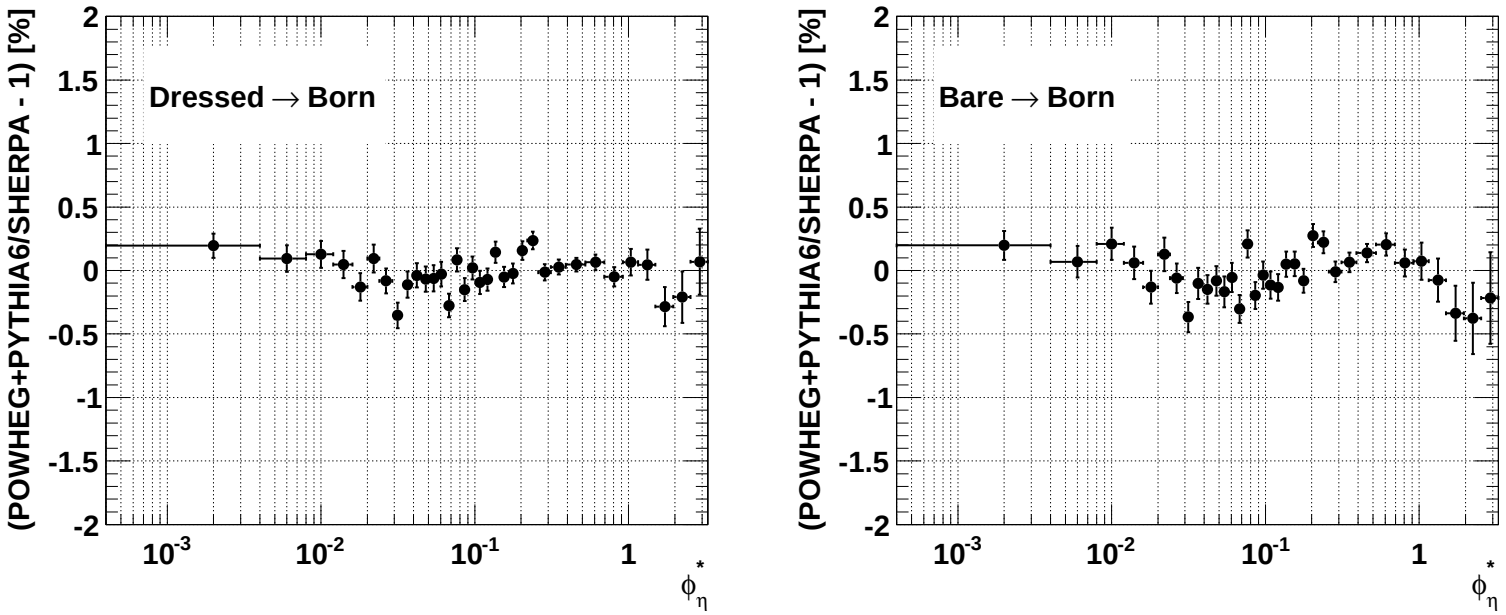

(a) (a)

(b) (b)

Figure 1: The difference of the QED FSR correction in PHOTOS and in SHERPA as a function of ϕ^*_η, for dressed leptons (a) and bare leptons (b). Corrections are calculated with respect to Born. Statistical uncertainties and acceptance cuts are **taken from CERN-THESIS-2013-001**.

Comparison plots taken from experiments

- The first results of ϕ^*_η measurements with ATLAS experiment were presented already. In that experimental publication the **systematic error of** 0.3% to ϕ^*_η due to implementation of QED final state radiation (FSR) in the applied Monte Carlo generators, was estimated in proportion of differences between PHOTOS+PYTHIA and SHERPA simulations:

  ATLAS Collaboration. *Measurement of angular correlations in Drell-Yan lepton pairs to probe Z/γ^* boson transverse momentum at $\sqrt{s} = 7$ TeV with the ATLAS detector* Phys.Lett. B720 (2013) 32.

- For me the plot from previous slide is a pointer to work performed by CDF, D0 and LHC experiments; esp. ATLAS and LHCb.

- Comparisons with HORACE on QED FSR, were performed by experiments as well.

- Principle of PHOTOS, HORACE and SHERPA algorithms for QED FSR are different. The comparisons are providing insight into the theoretical systematic error.

- Recently we have enriched these studies with SANC and KKMC comparisons.

- Sound estimation of systematic errors for each of these simulation algorithms/(program results) is important for high precision measurements.

Comparison plots taken from experiments

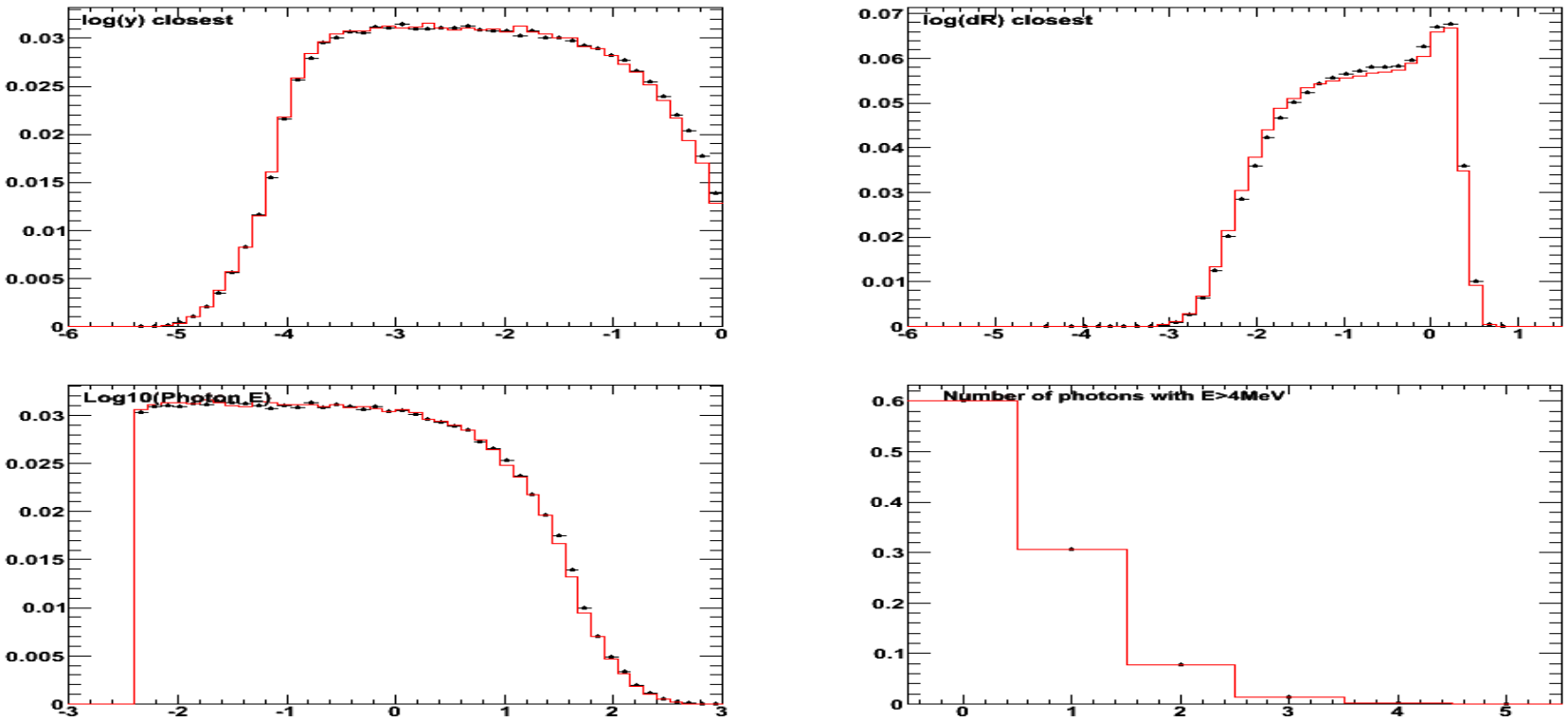

Comparison of PHOTOS *and* HORACE *for FSR in* $Z \to \mu^+\mu^-$ **(2010, private communication, CDF experiment)**.

This was my starting point for accessing QED uncertainties of W mass measurements. The studies for ϕ^*_η measurement followed.

Example of tests for theoretical uncertainties:

- I will present selected plots for comparisons of results from distinct programs.
- The purpose is to demonstrate that the agreements presented on plots used by experiments are based on much broader foundations.
- References to progams used in evaluation of th. syst. uncertainties:

1. PHOTOS P. Golonka and Z. Was, *Eur. Phys. J.* **C45** (2006) 97
2. KKMC S. Jadach, Z. Wąs and B. F. L. Ward, *Comput.Phys.Commun.* **130** (2000) 260
3. SHERPA T. Gleisberg *et al.*, *JHEP* **0902** (2009) 007
4. SANC A. Andonov *et al. Comput.Phys.Commun.* **174** (2006) 481
5. HORACE C. Carloni Calame,*JHEP* **0710** (2007) 109.
6. WINHAC W. Płaczek and S. Jadach, *Eur. Phys. J.* **C29** (2003) 325

Example of tests for theoretical uncertainties:

QED second order matrix element.

- Algoithms of KKMC and SHERPA are based on exclusive exponentiation. SHERPA features first order QED FSR matrix element only. The LEP legacy generator KKMC features second order matrix element as default.
- KKMC offers excellent benchmark for evaluating importance of the second order matrix element as it can be also downgraded to first order only.

  LIMITATION: at present it can be used only for fixed incoming quark momenta.

  Net effect of second order matrix element embedded in exclusive exponentiation can be calculated. **It is the only program available for this purpose.**

  We use this opportunity regularly for benchmarking PHOTOS, now we have used it for ϕ^*_η observable.

Example of tests for theoretical uncertainties:

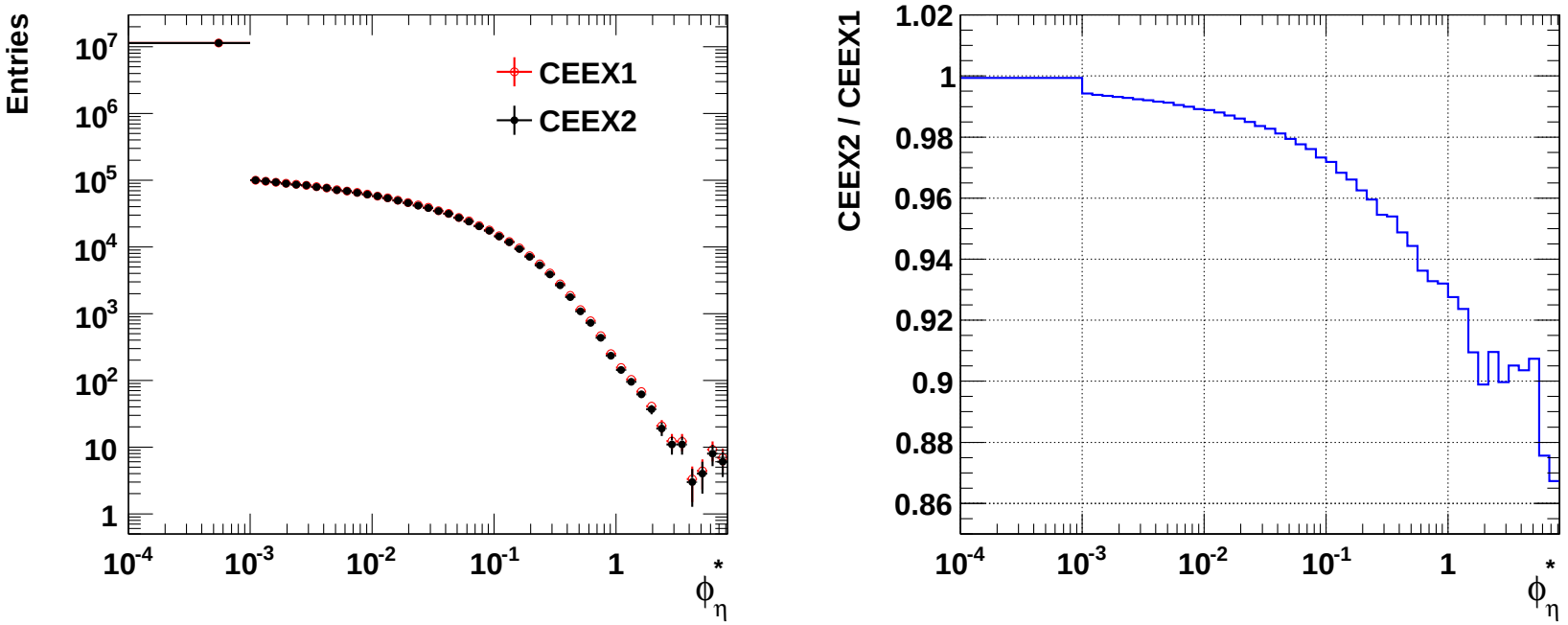

Figure 2: **arXiv:1303.2220**: the ϕ^*_η distribution: the comparisons of the CEEX2 and CEEX1 results. The sample of $u\bar{u} \to e^+e^-(n\gamma)$ events is generated. The virtuality of the Z boson equal to its mass is used. The boost to the laboratory frame of Z is performed prior to histogramming with cuts. The longitudinal momentum of Z is generated according to WINHAC in pp collision at $\sqrt{s} = 7$ TeV, while $p_T^Z = 0$. In the first bin, the configurations with ϕ^*_η smaller than 0.001 are collected.

Example of tests for theoretical uncertainties:

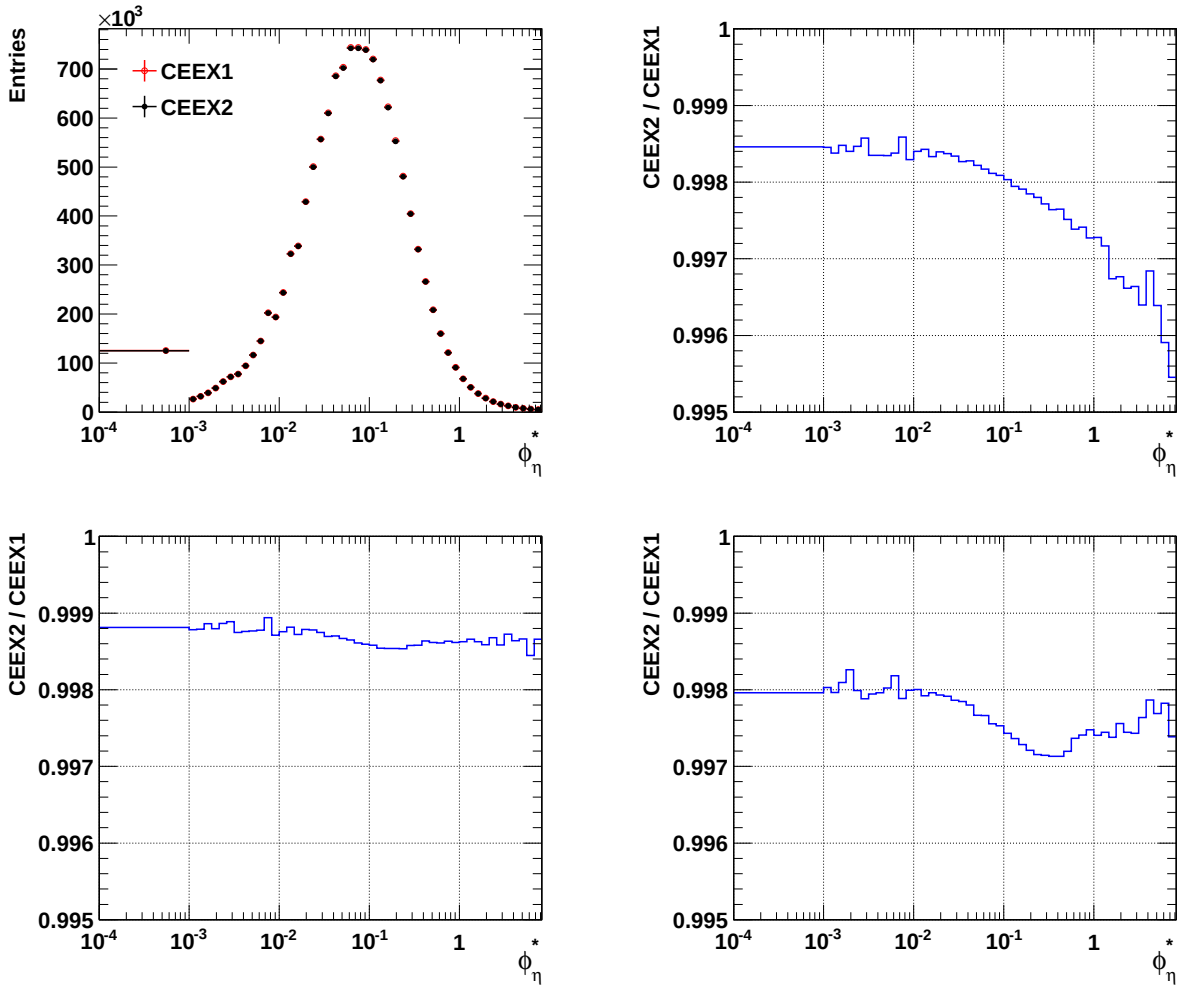

Figure 3: **arXiv:1303.2220**: the ϕ^*_η distribution: the comparisons of the CEEX2 and CEEX1 results. The $u\bar{u} \to e^+e^-(n\gamma)$ events. The boost to the laboratory frame of Z is performed prior to **histogramming with typical exp. cuts**. The plot with extra 66 GeV $< m_{ee} <$ 116 GeV is on the bottom-left side. Bottom-right side, in addition, events with the Z/γ^* virtuality of 115 GeV (instead of 92 GeV) are taken, a wavy structure appears.

Example of tests for theoretical uncertainties:

- The first results of ϕ^*_η measurements with ATLAS experiment quoted systematic error of 0.3% to ϕ^*_η due to implementation of QED final state radiation (FSR) in their Monte Carlo generators. It was estimated in proportion of differences observed between PHOTOS and SHERPA.

  ATLAS Collaboration. *Measurement of angular correlations in Drell-Yan lepton pairs to probe Z/γ^* boson transverse momentum at $\sqrt{s} = 7$ TeV with the ATLAS detector* Phys.Lett. B720 (2013) 32.

- **Thanks to the tests with KKMC we could confirm:** Missing in SHERPA second order matrix element of QED FSR is not a probem at precision level for ϕ^*_η of 0.3% .

- However, observed differences should be traced further. Missing terms will be needed when precision will improve further.

- There is room for improving TH precision on leptonic degrees of freedom! Total systematic error for luminosity (Bhabha scattering) at LEP reached 0.04%.

More on QED theoretical uncertainties:

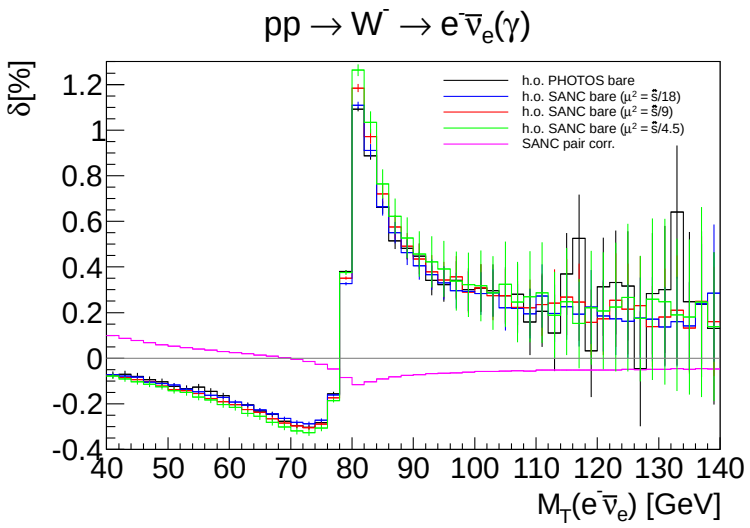

Figure 4: **arXiv:1212.6783**: *higher order photonic and pair corrections (δ in %) for basic distributions from* PYTHIA+PHOTOS *and* SANC *in $W^- \to e^- \bar{\nu}$ decay.*

In PHOTOS emission of additional pairs is not taken into account

Size of this missing effect has to be evaluated

Let me demonstrate just one plot prepared for that purpose on the basis of SANC generations

Effects are even smaller for ϕ^*_η and can be neglected for 0.3% precision level.

More on QED theoretical uncertainties:

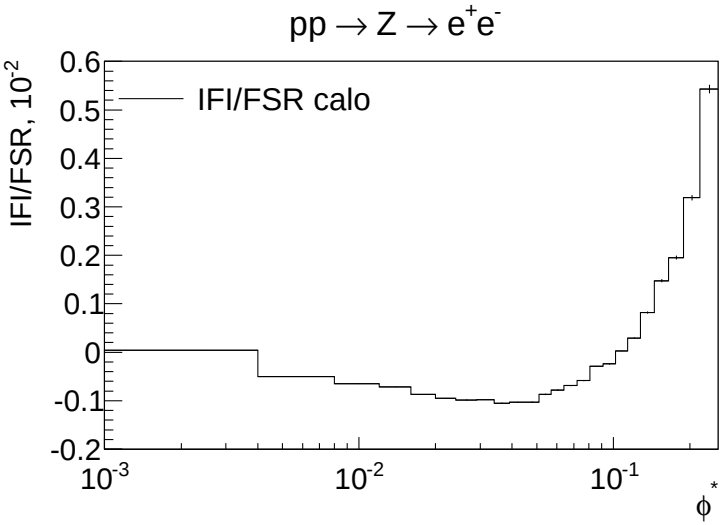

Figure 5: **arXiv:1212.6783***: IFI/FSR ratio in Z decay for ϕ^*_η distribution. For $\phi^*_\eta > 0.2$ interference effects become sizable.*

In PHOTOS only QED FSR emission is taken into account

ISR-FSR radiation interference is omitted

In general, this effect is expected to be of order of α_{QED} but for Z or W observables suppression factor $\frac{\Gamma}{M}$ is expected for large class of cuts

Effect is small, can be neglected for 0.3% precision level and present day selection cuts for ϕ^*_η.

It is important that proper calculation scheme is used. Mismatch between QED FSR and remaining genuine weak corrections must be avoided.

Standard tests

I have skipped presentation of standard tests, every Monte Carlo should be equipped with. We have emedded our main tests in special package MC-TESTER.

Test need to be performed for distinct distributions and distinct physics approximations used in the calculations.

For PHOTOS this include:

- Test of phase-space algorithm
- Comparisons with simulations at the fixed first order for Z and W decays. Precision $\simeq 10^{-4}$ was achieved.
- Comparisons at different level of matrix element sophistication: single photon emission, multiple photon emission, universal emission kernel, kernel featuring channel dependent matrix element.
- Comparisons with other simulations featuring multiphoton radiation. In most cases done with KKMC but also HORACE, SHERPA, WINHAC.

PHOTOS-QED-EW: short description

Presentation

- PHOTOS (by E.Barberio, B. van Eijk, Z. W., P.Golonka) is used to simulate the effect of radiatiative corrections in decays, since 1989.
- Full events combining complicated tree structure of production and subsequent decays have to be fed into PHOTOS, usually with the help of HEPEVT event record of F77 (or HepMC event record of C++).
- At every event decay tree branching, PHOTOS intervene. With certain probability extra photon(s) may be added and kinematics of other particles is then adjusted.
- The phase space is exact. For the matrix element truncations/approximations are used. That is why technique of correlated samples is possible.
- In general case universal kernel is used, but for the decays of Z or W, in the C++ applications, the kernel based on exact matrix element is available.
- In soft photon and collinear limits multiph. matrix elements approach exact ME.

PHOTOS-QED-EW: short presentation

Electroweak corrections $\longrightarrow$ *arXiv:1212.6783*

- QED FSR is well defined if one considers narrow resonace intermediate states
- Otherwise there is an ambiguity and risk of double counting of some contributions.
- This is specially important in case of charged W decay.
- Special tests and arrangements for compatibility with Electroweak calculations (where pure QED FSR must be switched off) are necssary for high precision applications.

For the sake of *tuned comparison* with PHOTOS, a special prescription for QED and genuine weak component separation[a] was introduced into SANC.

[a] This prescription should be respected also in electroweak, non-QED FSR calculations used together with PHOTOS in practical applications.

PHOTOS-QED-EW: short presentation

Electroweak corrections⟶ arXiv:1212.6783

Let us consider a formal separation of the pure weak (PW) and QED contributions δ^{PW} and δ^{QED} to the total W^+ decay width

$$\Gamma_W^{PW+QED} = \Gamma^{LO}(\delta^{PW} + \delta^{QED}). \quad (1)$$

This process is described by 6 QED-like diagrams with virtual photon line and 3 other ones with real photon emission which together lead to the formula

$$\delta^{QED} = \frac{\alpha}{\pi}\left[Q_W^2\left(\frac{11}{6} - \frac{\pi^2}{3}\right) + (Q_l^2)\left(\frac{11}{8} - \frac{3}{4}\log\frac{M_W^2}{\mu_{PW}^2}\right)\right],$$

where parameter μ_{PW} is the 't Hooft scale introduced for separation of QED and PW contributions. In order to separate the FSR QED contribution, we choose $\mu_{PW} = M_W \exp(-\frac{11}{12})$. This value of the 't Hooft scale makes the total QED contribution to the W boson decay being equal to zero. This is in agreement with the corresponding treatment in PHOTOS, where by construction the effect of FSR to a process does not change the normalization of the cross section.

PHOTOS-QED-EW: short presentation

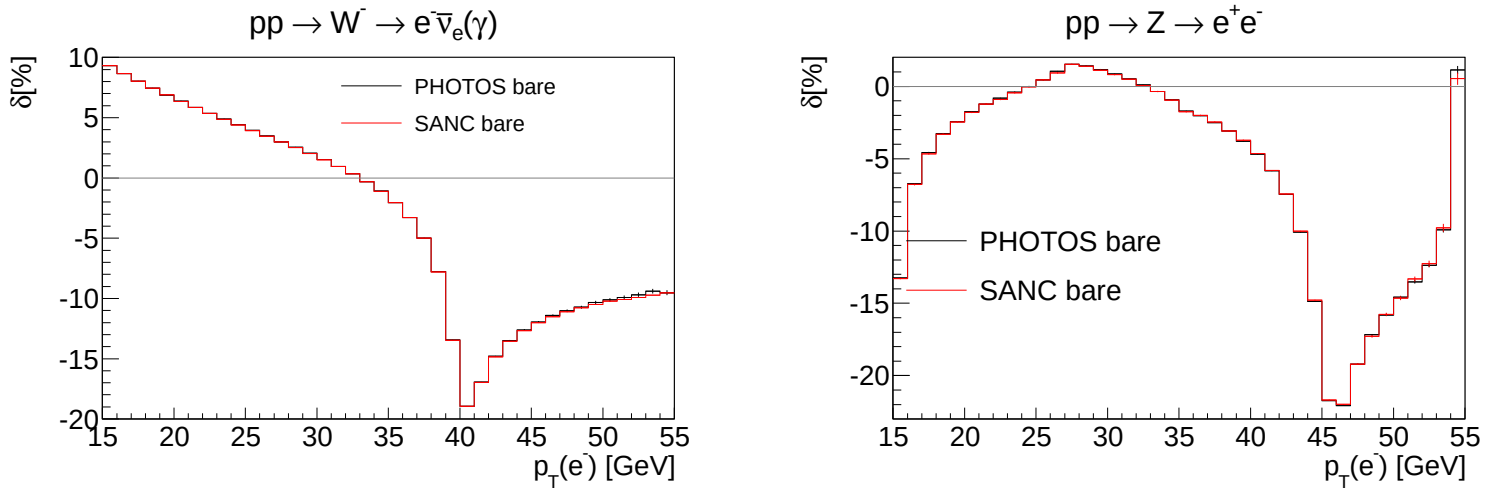

(a) (b)

Figure 6: $\mathcal{O}(\alpha)$ corrections for basic kinematical distributions from PYTHIA+PHOTOS and SANC in $W \to e\nu$ and in $Z \to ee$ decay.

bare = leptons not recobined with photons radiation.

Taken from arXiv:1212.6783 .

Summary

1. I hope I have explained some aspects of evaluation of theoretical systematic error fom QED FSR in observables such as ϕ^*_η.
2. My aim was to stress importance of taking into account particular experimental cuts...
3. ... but also theoretical basis: comparison of results at the distinct perturbation level, ...
4. ... also estimation of neglected effects: pairs, interference etc., which may depend on cuts.
5. In short: cooperation between experimental and theoretical physicists is crucial for exploring potential of precision measurements at LHC.
6. **I apologize for not showing here other tests performed by wide community of programs users.**

EXTRA SLIDES

Phase Space: toward factorization

Othodox Lorentz-invariant phase space (*Lips*) is in use in PHOTOS!

$$
\begin{aligned}
& dLips_{n+1}(P) = \\
& \frac{d^3k_1}{2k_1^0(2\pi)^3} \cdots \frac{d^3k_n}{2k_n^0(2\pi)^3} \frac{d^3q}{2q^0(2\pi)^3} (2\pi)^4 \delta^4\Big(P - \sum_1^n k_i - q\Big) \\
= \quad & d^4p\delta^4(P-p-q) \frac{d^3q}{2q^0(2\pi)^3} \frac{d^3k_1}{2k_1^0(2\pi)^3} \cdots \frac{d^3k_n}{2k_n^0(2\pi)^3} (2\pi)^4 \delta^4\Big(p - \sum_1^n k_i\Big) \\
= \quad & d^4p\delta^4(P-p-q) \frac{d^3q}{2q^0(2\pi)^3} dLips_n(p \to k_1 \ldots k_n).
\end{aligned}
$$

Integration variables, the four-vector p, compensated with $\delta^4\big(p - \sum_1^n k_i\big)$, and another integration variable M_1 compensated with $\delta\big(p^2 - M_1^2\big)$ are introduced.

Phase Space Formula of Photos

$$dLips_{n+1}(P \to k_1 ... k_n, k_{n+1}) = dLips_n^{+1\ tangent} \times W_n^{n+1},$$

$$dLips_n^{+1\ tangent} = dk_\gamma d\cos\theta d\phi \times dLips_n(P \to \bar{k}_1 ... \bar{k}_n),$$

$$\{k_1, \ldots, k_{n+1}\} = \mathbf{T}\big(k_\gamma, \theta, \phi, \{\bar{k}_1, \ldots, \bar{k}_n\}\big). \qquad (2)$$

1. One can verify that if $dLips_n(P)$ was exact, then this formula lead to exact parametrization of $dLips_{n+1}(P)$
2. Practical implementation: Take the configurations from n-body phase space.
3. Turn it back into some coordinate variables.
4. construct new kinematical configuration from all variables.
5. **Forget about temporary $k_\gamma \theta \phi$. From now on, only weight and four vectors count.**
6. A lot depend on $\mathbf{T}$. Options depend on matrix element: must tangent at singularities. Simultaneous use of several $\mathbf{T}$ is possible and necessary/convenient if more than one charge is present in final state.

Phase Space: (main formula)

If we choose

$$G_n \;:\; M^2_{2\ldots n}, \theta_1, \phi_1, M^2_{3\ldots n}, \theta_2, \phi_2, \ldots, \theta_{n-1}, \phi_{n-1} \;\rightarrow\; \bar{k}_1 \ldots \bar{k}_n \tag{3}$$

and

$$G_{n+1} \;:\; k_\gamma, \theta, \phi, M^2_{2\ldots n}, \theta_1, \phi_1, M^2_{3\ldots n}, \theta_2, \phi_2, \ldots, \theta_{n-1}, \phi_{n-1} \;\rightarrow\; k_1 \ldots k_n, k_{n+1} \tag{4}$$

then

$$\mathbf{T} = G_{n+1}(k_\gamma, \theta, \phi, G_n^{-1}(\bar{k}_1, \ldots, \bar{k}_n)). \tag{5}$$

The ratio of the Jacobians form the phase space weight W_n^{n+1} for the transformation. Such solution is universal and valid for any choice of G's. However, G_{n+1} and G_n has to match matrix element, otherwise algorithm will be inefficient (factor 10^{10} ...).

In case of PHOTOS G_n's

$$W_n^{n+1} = k_\gamma \frac{1}{2(2\pi)^3} \times \frac{\lambda^{1/2}(1, m_1^2/M^2_{1\ldots n}, M^2_{2\ldots n}/M^2_{1\ldots n})}{\lambda^{1/2}(1, m_1^2/M^2, M^2_{2\ldots n}/M^2)}, \tag{6}$$

Phase Space: (multiply iterated)

By iteration, we can generalize formula (2) and add l particles:

$$dLips_{n+l}(P \to k_1 ... k_n, k_{n+1} ... k_{n+l}) = \frac{1}{l!} \prod_{i=1}^{l} \left[dk_{\gamma_i} d\cos\theta_{\gamma_i} d\phi_{\gamma_i} W_{n+i-1}^{n+i} \right]$$

$$\times dLips_n(P \to \bar{k}_1 ... \bar{k}_n), \tag{7}$$

$$\{k_1, \ldots, k_{n+l}\} = \mathbf{T}\big(k_{\gamma_l}, \theta_{\gamma_l}, \phi_{\gamma_l}, \mathbf{T}\big(\ldots, \mathbf{T}\big(k_{\gamma_1}, \theta_{\gamma_1}, \phi_{\gamma_1}, \{\bar{k}_1, \ldots, \bar{k}_n\}\big) \ldots\big).$$

Note that variables $k_{\gamma_m}, \theta_{\gamma_m}, \phi_{\gamma_m}$ are used at a time of the $m-$th step of iteration only, and are not needed elsewhere in construction of the physical phase space; the same is true for invariants and angles $M^2_{2\ldots n}, \theta_1, \phi_1, \ldots, \theta_{n-1}, \phi_{n-1} \to \bar{k}_1 \ldots \bar{k}_n$ of (3,4), which are also redefined at each step of the iteration. Also intermediate steps require explicit construction of temporary $\bar{k}'_1 \ldots \bar{k}'_n \ldots \bar{k}'_{n+m}$, statistical factor $\frac{1}{l!}$ added.

We have got **exact distribution** of **weighted** events over $n + l$ body phase space.

Phase Sspace: next step.

Important points:

- Number of particles is phase space parameter too.
- Some particles can or even must be ignored:
  - Because they are not observed (neutrinos soft photons).
  - Because they are involved in soft cancellation.
- Lots of troubles and misunderstandings between experimental and theoretical physicists.
- **WARNING: theoretical calculation often have in mind inclusive quantities only. Intermediate steps look like 'prepared' for exlusive MC but not necessarily can be used that way!**

Pase Space: Trivial link to evolution equations used in benchmarks

- if c=0, $\lambda^{1/2}(a,b,c) := \sqrt{a^2+b^2+c^2-2ab-2ac-2bc} = |a-b|$

- If eg. in 3 body phase space invariant mass M of pair is used and third particle is masless then its energy k in rest frame: $k = \frac{S-M^2}{2\sqrt{S}}$.

- That is all what is needed from phase space jacobians for picture of structure functions. Rest belong to matrix elements.

- Side remark: This simplification is **not** used in PHOTOS, but it provides good way for getting benchmarks and can be used to show that PHOTOS sums up those terms which contribute to leading logarithms (of bremsstrahlung) to all orders.

Phase Space Formula: multichannels.

Often MC algorithm has to be split into branches. In the most general case, when n different parametrizations of the phase space with different orderings of particles are in use, the cross section can be written as follows:

$$d\Gamma_X = \sum_{\lambda=1}^{n} \int_0^1 \prod_{i=1}^{m} dx_i \; P_\lambda \left[\sum_{\delta=1}^{n} P_\delta J_\delta^{-1}(q_1(\lambda, x_i), ...q_k(\lambda, x_i)) \right]^{-1} \times |M|^2.$$

In the above formula the four-momenta $q_i(\lambda, x_i)$ are calculated from the random numbers x_i according to the parametrization of the phase space of type λ. The Jacobians J_δ have to be calculated for all parametrizations of the phase space at the point q_i; P_λ denotes the probability of choosing the parametrization of type λ in the generation, λ thus takes[a] a role of an additional discrete variable in the generation. Numerical values of probabilities P_λ do not affect the final distributions, but only the efficiency of the generation.

[a] But not δ.

Phase Space case of complex singularity structure

- Several G_{n+1} can be used simultaneously (branching of the generation algorithm).
- Each G_{n+1} can be used presample distinct singularities.
- The price: W_n^{n+1} is more complicated but all remain exact.
- HOWEVER: We have observed that while matching Jacobians for the two branches related to collinear singularity of photons along direction of l^+ and l^+ (in Z decay) approximation must be used if more than one photon is present in final state. Otherwise solution become inconsistent. Phase space is not iterative, whereas matrix element for multiphoton state is obtained by iteration.
- AVOID INOCONSISTENCY: in expanding manifold curvature: must be the same for phase space and Matrix Element. Phase space is manifold, Matrix element squared – bilinear form on it. Truncation of perturbative expansion or iterative solutions mean truncation in powers of Ricci tensor, this has to be consistent. Multichannel phase space is not iterative, single branch algorithm we explained before is that is OK for expansion and exact phasese space remain. I have learned that hard way.

Phase Space: (multiply iterated)

We have generalized formula phase space formula to case of l particles added:

$$dLips_{n+l}(P \to k_1 ... k_n, k_{n+1} ... k_{n+l}) = \frac{1}{l!} \prod_{i=1}^{l} \left[dk_{\gamma_i} d\cos\theta_{\gamma_i} d\phi_{\gamma_i} W_{n+i-1}^{n+i} \right]$$

$$\times dLips_n(P \to \bar{k}_1 ... \bar{k}_n), \tag{8}$$

$$\{k_1, \ldots, k_{n+l}\} = \mathbf{T}\big(k_{\gamma_l}, \theta_{\gamma_l}, \phi_{\gamma_l}, \mathbf{T}\big(\ldots, \mathbf{T}\big(k_{\gamma_1}, \theta_{\gamma_1}, \phi_{\gamma_1}, \{\bar{k}_1, \ldots, \bar{k}_n\}\big) \ldots\big).$$

Now we have to start talking about matrix elements: Our relation between n and n+l body phase space is motivated by cancellation of infrared singulatrites. It provides kind of triangulation. Measure defining distance between points from manifolds of distinct no. of particles. Such phase space points are close if they differ by presence of soft photons only.

Experimental user attention necessary. Can 1 GeV photon be ignored or only 0.1 MeV one.

We will move now from **exact distribution** of **weighted** events over $n + l$ body phase space to case where l is parameter too, but all remain exact!

Crude Ddistribution and crude matrix element

If we add arbitrary factors $f(k_{\gamma_i},\theta_{\gamma_i},\phi_{\gamma_i})$ and sum over l we obtain:

$$\sum_{l=0}\exp(-F)\frac{1}{l!}\prod_{i=1}^{l} f(k_{\gamma_i},\theta_{\gamma_i},\phi_{\gamma_i})dLips_{n+l}(P\to k_1...k_n,k_{n+1}...k_{n+l}) =$$

$$\sum_{l=0}\exp(-F)\frac{1}{l!}\prod_{i=1}^{l}\left[f(k_{\gamma_i},\theta_{\gamma_i},\phi_{\gamma_i})dk_{\gamma_i}d\cos\theta_{\gamma_i}d\phi_{\gamma_i}W_{n+i-1}^{n+i}\right]\times$$

$$dLips_n(P\to\bar{k}_1...\bar{k}_n), \qquad (9)$$

$$\{k_1,\ldots,k_{n+l}\}=\mathbf{T}\big(k_{\gamma_l},\theta_{\gamma_l},\phi_{\gamma_l},\mathbf{T}\big(\ldots,\mathbf{T}\big(k_{\gamma_1},\theta_{\gamma_1},\phi_{\gamma_1},\{\bar{k}_1,\ldots,\bar{k}_n\}\big)\ldots\big),$$

$$F=\int_{k_{min}}^{k_{max}} dk_\gamma d\cos\theta_\gamma d\phi_\gamma f(k_\gamma,\theta_\gamma,\phi_\gamma). \leftarrow \text{KLN good start}$$

- The olive parts of rhs. alone, give crude distribution over tangent space (orthogonal set of variables k_i,θ_i,ϕ_i). We restrict phase space by k_{min} (typically 10^{-6} but not by k_{max}.

- Factors f must be integrable over tangent space. Regulators of singularities necessary.

- We requested

$$\sigma_{tangent} = 1 =$$

$$\sum_{l=0} \exp(-F) \frac{1}{l!} \prod_{i=1}^{l} \left[f(k_{\gamma_i}, \theta_{\gamma_i}, \phi_{\gamma_i}) dk_{\gamma_i} d\cos\theta_{\gamma_i} d\phi_{\gamma_i} \right]$$

Because of Kinoshita Lee Nauenberg theorem we know that exact calculation of the cross section give result of similar property. We get another element of PHOTOS basis.

- For precise predictions, real emission and virtual corrections need to be calculated and their factorization properties analyzed.

- Choice of f must be synchronized so correcting weights for matrix elements do not fluctuate wildely.

Heuristic CW complexes

We define our crude distribution over yellow space (surface=1) (reprersented by sum of: red point, green lines and flat yellow square), then we do projections using transformation T and matrix lements.

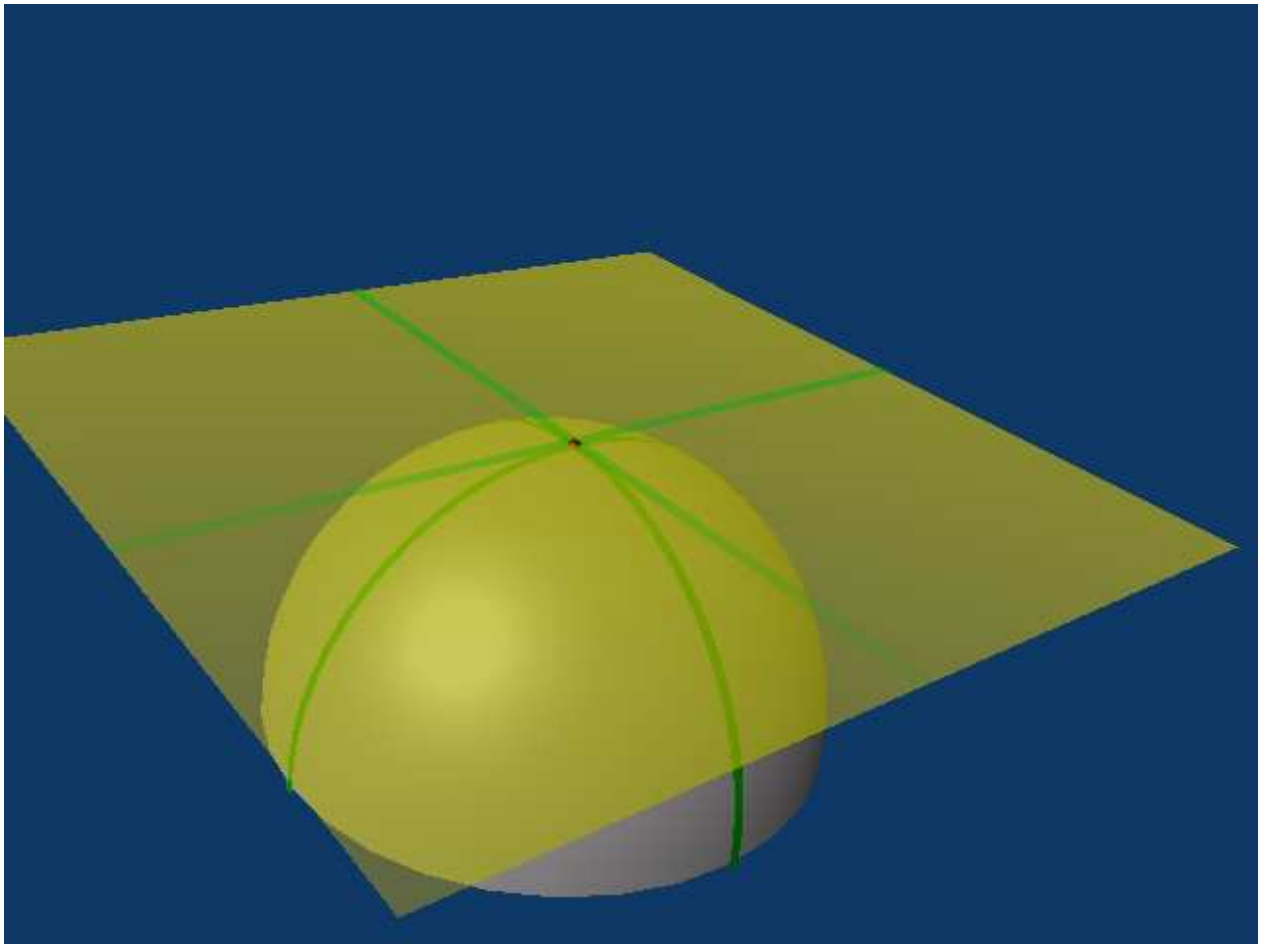

Heuristic CW complexes projection step 1

We project in steps, relative measure of point and lines on cylinder is larger than in previous step, overall measure remain 1.

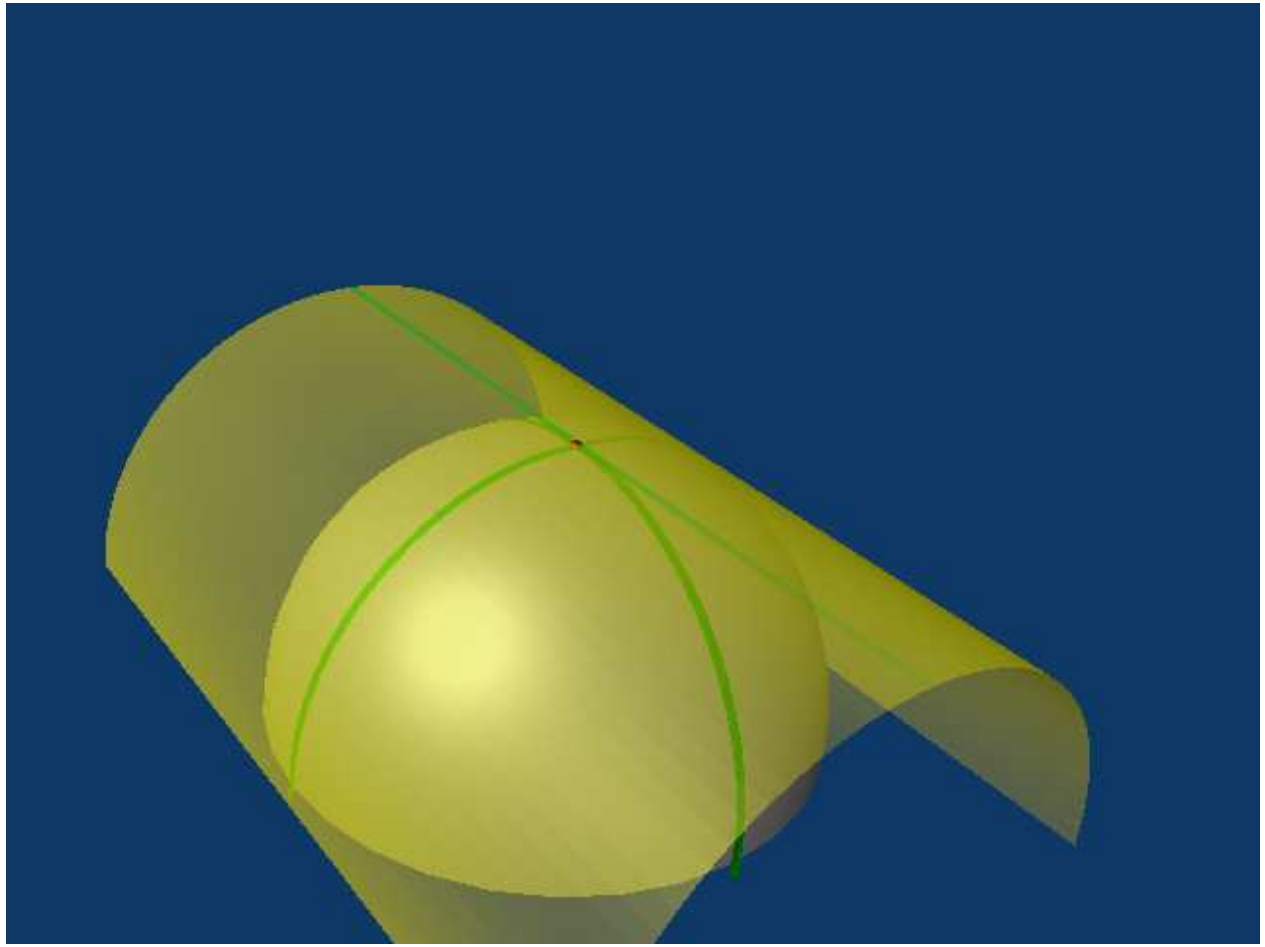

Heuristic CW complexes projection step 2

Final distribution does not match the exact one, solely because approximation in matrix elements, phase space is exact.

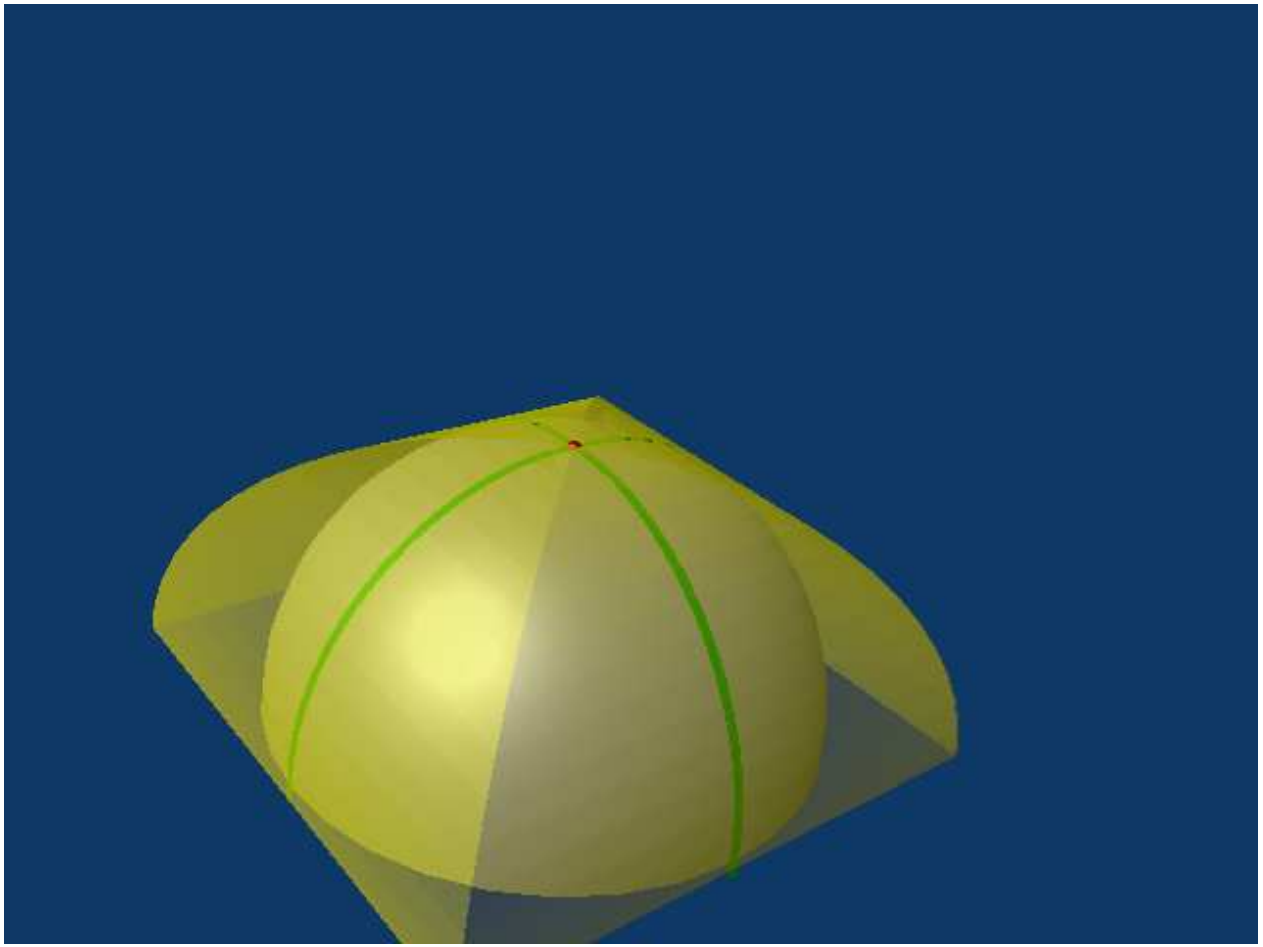

Construction elements summary

- we defined eqivalence of some n- and $(n+l)$-body ph. space points
- triangulation (CW-complexes) resulting from phase space parametrizations match structure of singularities.
- such CW-complexes for exact space and tangent space match
- to achieve that we could use properties of factorization as known in QED, guessed in scalar QED, what about QCD?
- infrared singularity being within perturbative domain was a bonus.
- we studied (1982-2008) properties of cross sections and later also spin amplitudes: distinct processes.
- formulas for virtual corrections more often than real emissions could be taken from other people works in unchanged form.
- M.E. content of CEEX-YFS exponentiation is my basis $\longrightarrow$ benchmarks too.

Matrix Element (starting point):

- Directly starting from Feynman rules one can calculate spin amplitude for any QED/QCD process.
- The case of $Z \to l^+ l^- \gamma$ is the backbone of PHOTOS design
- single photon amplitude(momentum k_1 polarization e_1 fermion spinors $u(p)$ and $v(q)$ dropped):

$$I = \not{J}\left[\left(\frac{p\cdot e_1}{p\cdot k_1} - \frac{q\cdot e_1}{q\cdot k_1}\right)\right] - \left[\frac{1}{2}\frac{\not{e}_1\not{k}_1}{p\cdot k_1}\right]\not{J} + \not{J}\left[\frac{1}{2}\frac{\not{e}_1\not{k}_1}{q\cdot k_1}\right]$$

three gauge invariant parts: appear in other processes too

Pre-property for factorizations of any sorts... but must be deciphered

- The fully differential distribution from MUSTRAAL (used also in KORALZ for single photon mode) reads:

$$X_f = \frac{Q'^2\alpha(1-\Delta)}{4\pi^2 s}s^2 \quad \left\{ \frac{1}{(k'_+k'_-)}\left[\frac{\mathrm{d}\sigma_B}{\mathrm{d}\Omega}(s,t,u') + \frac{\mathrm{d}\sigma_B}{\mathrm{d}\Omega}(s,t',u)\right]\right\}$$

- Here:

$$\begin{aligned} s &= 2p_+\cdot p_-, \quad & s' &= 2q_+\cdot q_-, \\ t &= 2p_+\cdot q_+, \quad & t' &= 2p_+\cdot q_-, \\ u &= 2p_+\cdot q_-, \quad & u' &= 2_-\cdot q_+, \\ k'_\pm &= q_\pm\cdot k, \quad & x_k &= 2E_\gamma/\sqrt{s} \end{aligned}$$

- The Δ term is responsable for final state mass dependent terms, p_+, p_-, q_+, q_-, k denote four-momenta of incoming positron, electron beams, outcoming muons and bremsstrahlung photon.

- after trivial manipulation it can be written as:

$$X_f = \frac{Q'^2\alpha(1-\Delta)}{4\pi^2 s}s^2 \quad \left\{ \frac{1}{(k'_+ + k'_-)}\frac{1}{k'_-}\left[\frac{\mathrm{d}\sigma_B}{\mathrm{d}\Omega}(s,t,u') + \frac{\mathrm{d}\sigma_B}{\mathrm{d}\Omega}(s,t',u)\right] \right.$$
$$\left. + \frac{1}{(k'_+ + k'_-)}\frac{1}{k'_+}\left[\frac{\mathrm{d}\sigma_B}{\mathrm{d}\Omega}(s,t,u') + \frac{\mathrm{d}\sigma_B}{\mathrm{d}\Omega}(s,t',u)\right] \right\}$$

- In PHOTOS the following expression is used in universal application (AP adj.):

$$X_f^{PHOTOS} = \frac{Q'^2\alpha(1-\Delta)}{4\pi^2 s}s^2 \left\{ \right.$$
$$\frac{1}{k'_+ + k'_-}\frac{1}{k'_-} \left[(1+(1-x_k)^2)\frac{\mathrm{d}\sigma_B}{d\Omega}\left(s, \frac{s(1-\cos\Theta_+)}{2}, \frac{s(1+\cos\Theta_+)}{2}\right)\right]\frac{(1+\beta\cos\Theta_\gamma)}{2}$$
$$\left. + \frac{1}{k'_+ + k'_-}\frac{1}{k'_+} \left[(1+(1-x_k)^2)\frac{\mathrm{d}\sigma_B}{d\Omega}\left(s, \frac{s(1-\cos\Theta_-)}{2}, \frac{s(1+\cos\Theta_-)}{2}\right)\right]\frac{(1-\beta\cos\Theta_\gamma)}{2} \right\}$$

$$\text{where}: \Theta_+ = \angle(p_+, q_+),\ \Theta_- = \angle(p_-, q_-)$$

$\Theta_\gamma = \angle(\gamma, \mu^-)$ are defined in (μ^+, μ^-)-pair rest frame

The matrix element weight

- weight for exact matrix element is easy to implement $WT = X_f / X_f^{PHOTOS}$
- also factor $\Gamma^{total}/\Gamma^{Born} = 1 + \frac{3}{4}\frac{\alpha}{\pi}$ defines first order weight, it depends on virtual corrections if non leading mass terms are kept.
- $WT = \frac{X_f}{X_f^{PHOTOS}} \frac{\Gamma^{Born}}{\Gamma^{total}}$

The differences of X_f and X_f^{PHOTOS} are important

- Without process dependent weight PHOTOS is universal and can be combined with any generator rather easily, thus 300+ citations. Last year mainly for B decays and measurements of quark mixing angles.
- Photos weight is then process independent.
- Virtual corrections for decays like $K^+ \to \pi^+\pi^- l^+ \nu_l$ more complicated than

overall constant. Recent paper by Kuraev et al. (2009) $\longrightarrow$ next step.

Matrix Element (anything in common?):

- We have seen nice properties of matrix element squared which were factorizing into Born-like distribution and photon factor.
- It was shown many years ago by Ronald Kleiss that such property of distributions does not hold beyond first order!
- Dead end? Not really, just complex weights[a]
- single photon amplitude again:

$$I = \not{J}\left[\left(\frac{p\cdot e_1}{p\cdot k_1} - \frac{q\cdot e_1}{q\cdot k_1}\right)\right] - \left[\frac{1}{2}\frac{\not{e}_1\not{k}_1}{p\cdot k_1}\right]\not{J} + \not{J}\left[\frac{1}{2}\frac{\not{e}_1\not{k}_1}{q\cdot k_1}\right]$$

three gauge invariant parts, first is eikonal, other for collinear configuration along q and p

We look for these parts in higher order amplitudes

[a] Also: samples at different level of spophistication can be correlated up to NLO level. That is enough for most of experimental techniques, precision of correlated programs can be higher.

Matrix Element (double emission):

- The structure of exact spin amplitude for single emission looks promising.
- How does it translate to distributions?
- Does it extend to other processes, intercations? Scalar QED QCD as well?
- Does it extent to higher orders?
- Can one decipher anything without enforcing some phase space conditions?
- To identify the building blocks we have used gauge invariance, and we have used also segments localized at lower order.
- For tree diagrams gauge invariance mean in practice that replacement $k \longrightarrow e$ set experession to zero
- Virtual corrections add complication because of regularization schemes, we will skip that now.

Exact Matrix Element: $e^+e^- \to \nu_\mu \bar{\nu}_\mu \gamma\gamma$ *explicitly;*

- Expressions are valid for any current J,
- For complete amplitude add fermionic fields, eg. $\bar{u}(p)$ and $v(q)$; 1-st/2-nd photon momenta/polarizations are: k_1/k_2 e_1/e_2.

$$I_1^{\{1,2\}} = \frac{1}{2} \not{J} \left(\frac{p\cdot e_1}{p\cdot k_1} - \frac{q\cdot e_1}{q\cdot k_1} \right) \left(\frac{p\cdot e_2}{p\cdot k_2} - \frac{q\cdot e_2}{q\cdot k_2} \right) \qquad eikonal$$

$$I_{2l}^{\{1,2\}} = -\frac{1}{4} \left[\left(\frac{p\cdot e_1}{p\cdot k_1} - \frac{q\cdot e_1}{q\cdot k_1} \right) \frac{\not{e}_2 \not{k}_2}{p\cdot k_2} + \left(\frac{p\cdot e_2}{p\cdot k_2} - \frac{q\cdot e_2}{q\cdot k_2} \right) \frac{\not{e}_1 \not{k}_1}{p\cdot k_1} \right] \not{J} \qquad \beta_1$$

$$I_{2r}^{\{1,2\}} = \frac{1}{4} \not{J} \left[\left(\frac{p\cdot e_1}{p\cdot k_1} - \frac{q\cdot e_1}{q\cdot k_1} \right) \frac{\not{k}_2 \not{e}_2}{q\cdot k_2} + \left(\frac{p\cdot e_2}{p\cdot k_2} - \frac{q\cdot e_2}{q\cdot k_2} \right) \frac{\not{k}_1 \not{e}_1}{q\cdot k_1} \right] \qquad \beta_1$$

$$I_3^{\{1,2\}} = -\frac{1}{8} \left(\frac{\not{e}_1 \not{k}_1}{p\cdot k_1} \not{J} \frac{\not{k}_2 \not{e}_2}{q\cdot k_2} + \frac{\not{e}_2 \not{k}_2}{p\cdot k_2} \not{J} \frac{\not{k}_1 \not{e}_1}{q\cdot k_1} \right) \qquad start for \beta_2 ...$$

$$I_{4p}^{\{1,2\}} = \frac{1}{8}\,\frac{1}{p\cdot k_1 + p\cdot k_2 - k_1\cdot k_2}\left(\frac{\not\epsilon_1\not k_1\not\epsilon_2\not k_2}{p\cdot k_1} + \frac{\not\epsilon_2\not k_2\not\epsilon_1\not k_1}{p\cdot k_2}\right)\not J$$

$$I_{4q}^{\{1,2\}} = \frac{1}{8}\not J\,\frac{1}{q\cdot k_1 + q\cdot k_2 - k_1\cdot k_2}\left(\frac{\not k_2\not\epsilon_2\not k_1\not\epsilon_1}{q\cdot k_1} + \frac{\not k_1\not\epsilon_1\not k_2\not\epsilon_2}{q\cdot k_2}\right)$$

$$I_{5pA}^{\{1,2\}} = \frac{1}{2}\not J\,\frac{k_1\cdot k_2}{p\cdot k_1 + p\cdot k_2 - k_1\cdot k_2}\left(\frac{p\cdot e_1}{p\cdot k_1} - \frac{k_2\cdot e_1}{k_2\cdot k_1}\right)\left(\frac{p\cdot e_2}{p\cdot k_2} - \frac{k_1\cdot e_2}{k_1\cdot k_2}\right)$$

$$I_{5pB}^{\{1,2\}} = -\frac{1}{2}\not J\,\frac{1}{p\cdot k_1 + p\cdot k_2 - k_1\cdot k_2}\left(\frac{k_1\cdot e_2 k_2\cdot e_1}{k_1\cdot k_2} - e_1\cdot e_2\right)$$

$$I_{5qA}^{\{1,2\}} = \frac{1}{2}\not J\,\frac{k_1\cdot k_2}{q\cdot k_1 + q\cdot k_2 - k_1\cdot k_2}\left(\frac{q\cdot e_1}{q\cdot k_1} - \frac{k_2\cdot e_1}{k_2\cdot k_1}\right)\left(\frac{q\cdot e_2}{q\cdot k_2} - \frac{k_1\cdot e_2}{k_1\cdot k_2}\right)$$

$$I_{5qB}^{\{1,2\}} = -\frac{1}{2}\not J\,\frac{1}{q\cdot k_1 + q\cdot k_2 - k_1\cdot k_2}\left(\frac{k_1\cdot e_2 k_2\cdot e_1}{k_1\cdot k_2} - e_1\cdot e_2\right)$$

$$I_{6B}^{\{1,2\}} = -\frac{1}{4}\,\frac{k_1\cdot k_2}{p\cdot k_1 + p\cdot k_2 - k_1\cdot k_2}\left[+\left(\frac{p\cdot e_1}{p\cdot k_1} - \frac{k_2\cdot e_1}{k_1\cdot k_2}\right)\frac{\not\epsilon_2\not k_2}{p\cdot k_2} + \left(\frac{p\cdot e_2}{p\cdot k_2} - \frac{k_1\cdot e_2}{k_1\cdot k_2}\right)\frac{\not\epsilon_1\not k_1}{p\cdot k_1}\right]\not J$$

$$I_{7B}^{\{1,2\}} = -\frac{1}{4}\not{J}\frac{k_1\cdot k_2}{q\cdot k_1 + q\cdot k_2 - k_1\cdot k_2}\left[+\left(\frac{q\cdot e_1}{q\cdot k_1}-\frac{k_2\cdot e_1}{k_1\cdot k_2}\right)\frac{\not{k}_2\not{e}_2}{q\cdot k_2}+\left(\frac{q\cdot e_2}{q\cdot k_2}-\frac{k_1\cdot e_2}{k_1\cdot k_2}\right)\frac{\not{k}_1\not{e}_1}{q\cdot k_1}\right]$$

- for the **exponentiation** we have used **separation** into 3 parts only. It is **crystal clear**, also in case of contributions with t-channel W, was very useful for KKMC,
- for PHOTOS kernel, parts $I_3^{\{1,2\}}$, $I_{4p}^{\{1,2\}}$, $I_{4q}^{\{1,2\}}$ were studied separately as well.
- In fact older works on spin amplitdues wre used E. Richter-Was Z.Phys.C64:227-240,1994, Z.Phys.C61:323-340,1994.
- Clearly visible but not used for PHOTOS further separation of β_2 terms ...
- Presented above properties of spin amplitudes were used for PHOTOS design to make a choice of phase space parametrization and iteration of consecutive emission kernels that respect numerically as much as possible results of second order amplitudes. Also one want to remain consistent with NLO and exponentiation to all orders.

Matrix Element: $q\bar{q} \to Jgg$ - part proportional to $T^A T^B$ fermion spinors dropped

$$I_{lr}^{(1,2)} = \left(\frac{p\cdot e_1}{p\cdot k_1} - \frac{k_2\cdot e_1}{k_2\cdot k_1} - \frac{\not e_1 \not k_1}{2p\cdot k_1}\right) \not J \left(\frac{\not k_2 \not e_2}{2q\cdot k_2} + \frac{k_1\cdot e_2}{k_1\cdot k_2} - \frac{q\cdot e_2}{q\cdot k_2}\right)$$

$$I_{ll}^{(1,2)} = \frac{p\cdot k_2}{p\cdot k_1 + p\cdot k_2 - k_1\cdot k_2} \left(\frac{p\cdot e_1}{p\cdot k_1} - \frac{k_2\cdot e_1}{k_2\cdot k_1} - \frac{\not e_1 \not k_1}{2p\cdot k_1}\right) \left(\frac{p\cdot e_2}{p\cdot k_2} - \frac{k_1\cdot e_2}{k_1\cdot k_2} - \frac{\not e_2 \not k_2}{2p\cdot k_2}\right) \not J$$

$$I_{rr}^{(1,2)} = \not J \frac{q\cdot k_1}{q\cdot k_1 + q\cdot k_2 - k_1\cdot k_2} \left(\frac{q\cdot e_1}{q\cdot k_1} - \frac{k_2\cdot e_1}{k_2\cdot k_1} - \frac{\not k_1 \not e_1}{2q\cdot k_1}\right) \left(\frac{q\cdot e_2}{q\cdot k_2} - \frac{k_1\cdot e_2}{k_1\cdot k_2} - \frac{\not k_2 \not e_2}{2q\cdot k_2}\right)$$

$$I_{e}^{(1,2)} = \not J \left(1 - \frac{p\cdot k_2}{p\cdot k_1 + p\cdot k_2 - k_1\cdot k_2} - \frac{q\cdot k_1}{q\cdot k_1 + q\cdot k_2 - k_1\cdot k_2}\right) \left(\frac{k_1\cdot e_2}{k_1\cdot k_2}\ \frac{k_2\cdot e_1}{k_1\cdot k_2} - \frac{e_1\cdot e_2}{k_1\cdot k_2}\right)$$

Remainder:

$$I_{p}^{(1,2)} = -\frac{1}{4}\ \frac{1}{p\cdot k_1 + p\cdot k_2 - k_1\cdot k_2} \left(\frac{\not e_1 \not k_1 \not e_2 \not k_2 - \not e_2 \not k_2 \not e_1 \not k_1}{k_1\cdot k_2}\right) \not J$$

$$I_{q}^{(1,2)} = -\frac{1}{4}\ \not J\ \frac{1}{q\cdot k_1 + q\cdot k_2 - k_1\cdot k_2} \left(\frac{\not k_1 \not e_1 \not k_2 \not e_2 - \not k_2 \not e_2 \not k_1 \not e_1}{k_1\cdot k_2}\right)$$

Matrix Element: $q\bar{q} \to Jgg$ - part proportional to $T^B T^A$ fermion spinors dropped

$$I^{(2,1)}_{lr} = \left(\frac{p\cdot e_2}{p\cdot k_2} - \frac{k_1\cdot e_2}{k_1\cdot k_2} - \frac{\not e_2 \not k_2}{2p\cdot k_2}\right) \not J \left(\frac{\not k_1 \not e_1}{2q\cdot k_1} + \frac{k_2\cdot e_1}{k_2\cdot k_1} - \frac{q\cdot e_1}{q\cdot k_1}\right)$$

$$I^{(2,1)}_{ll} = \frac{p\cdot k_1}{p\cdot k_2 + p\cdot k_1 - k_2\cdot k_1} \left(\frac{p\cdot e_2}{p\cdot k_2} - \frac{k_1\cdot e_2}{k_1\cdot k_2} - \frac{\not e_2 \not k_2}{2p\cdot k_2}\right) \left(\frac{p\cdot e_1}{p\cdot k_1} - \frac{k_2\cdot e_1}{k_2\cdot k_1} - \frac{\not e_1 \not k_1}{2p\cdot k_1}\right) \not J$$

$$I^{(2,1)}_{rr} = \not J \frac{q\cdot k_2}{q\cdot k_2 + q\cdot k_1 - k_2\cdot k_1} \left(\frac{q\cdot e_2}{q\cdot k_2} - \frac{k_1\cdot e_2}{k_1\cdot k_2} - \frac{\not k_2 \not e_2}{2q\cdot k_2}\right) \left(\frac{q\cdot e_1}{q\cdot k_1} - \frac{k_2\cdot e_1}{k_2\cdot k_1} - \frac{\not k_1 \not e_1}{2q\cdot k_1}\right)$$

$$I^{(2,1)}_{e} = \not J \left(1 - \frac{p\cdot k_1}{p\cdot k_2 + p\cdot k_1 - k_2\cdot k_1} - \frac{q\cdot k_2}{q\cdot k_2 + q\cdot k_1 - k_2\cdot k_1}\right) \left(\frac{k_2\cdot e_1}{k_2\cdot k_1} \frac{k_1\cdot e_2}{k_2\cdot k_1} - \frac{e_2\cdot e_1}{k_2\cdot k_1}\right)$$

$$I^{(2,1)}_{p} = -\frac{1}{4} \frac{1}{p\cdot k_2 + p\cdot k_1 - k_2\cdot k_1} \left(\frac{\not e_2 \not k_2 \not e_1 \not k_1 - \not e_1 \not k_1 \not e_2 \not k_2}{k_2\cdot k_1}\right) \not J$$

$$I^{(2,1)}_{q} = -\frac{1}{4} \not J \frac{1}{q\cdot k_2 + q\cdot k_1 - k_2\cdot k_1} \left(\frac{\not k_2 \not e_2 \not k_1 \not e_1 - \not k_1 \not e_1 \not k_2 \not e_2}{k_2\cdot k_1}\right)$$

For QCD we have separation too; 12 gauge invariant parts

- Terms like

$$\left(\frac{p\cdot e_1}{p\cdot k_1}-\frac{k_2\cdot e_1}{k_2\cdot k_1}-\frac{\not{e}_1\not{k}_1}{2p\cdot k_1}\right) \qquad A$$

once integrated over part of phase space give Atarelli-Parisi kernel

- Terms

$$\frac{q\cdot k_1}{q\cdot k_1+q\cdot k_2-k_2\cdot k_1} \qquad B$$

if combined with phase space Jacobians can be used to redefine fermionic fields from $v(q)$ to $v(q-k_2)$ for example. Term of such type appeared already in scalar QED (normalization of hadronic current).

- No QCD prototype, for amplitudes $\longrightarrow$ my paper with A. van Hameren.

- For studies of amplitudes used in PHOTOS see my papers with: P. Golonka, G. Nanava (Z W H decays), G.Nanava Qinjun Xy (B γ^* decays), soon $K^{\pm}\longrightarrow l^{\pm}\nu\pi^+\pi^-$.

PHOTOS: short presentation

Presentation

- PHOTOS (by E.Barberio, B. van Eijk, Z. W., P.Golonka) is used to simulate the effect of radiatiative corrections in decays, since 1989.
- Full events combining complicated tree structure of production and subsequent decays have to be fed into PHOTOS, usually with the help of HEPEVT event record of F77 (beta version working with HepMC event record of C++ exist).
- This is often source of technical difficulties as standard is often overruled. Also numerical precision may be an issue.
- At every event decay branching, PHOTOS intervene. With certain probability extra photon may be added and kinematics of other particles adjusted.
- PHOTOS works on four-momenta double precision four-vectors. This creates some ‘fun’ with numerical stability.
- I will not talk about those time consuming aspects and my frustrations ...

Main References

- E. Barberio and Z. Was, Comput. Phys. Commun. **79**, 291 (1994).

  E. Barberio, B. van Eijk and Z. Was, Comput. Phys. Commun. **66**, 115 (1991).

- Z. Was, Eur. Phys. J. C **44** (2005) 489

- P. Golonka and Z. Was, Eur. Phys. J. C **45** (2006) 97, ibid, C50:53-62,2007

- G. Nanava, Z. Was, Eur.Phys.J.C51:569-583,2007

- G. Nanava, Z. Was, Q. Xu Matching NLO parton shower matrix element with exact phase space: Case of W —> l nu(gamma) and gamma* —> pi+ pi -(gamma),arXiv:0906.4052.

Problems With Event Record

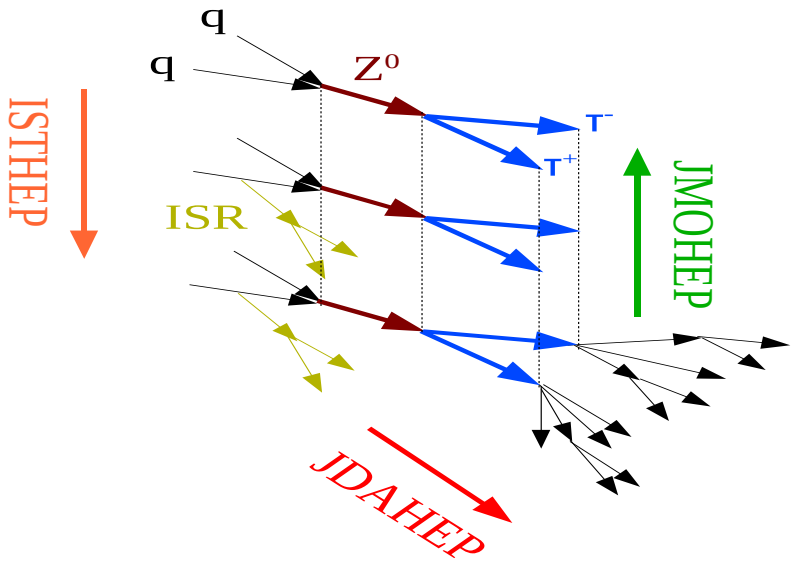

1. Hard process
2. with shower
3. after hadronization
4. Event record overloaded with physics beyond design ⟶ gramar problems.
5. That is potential problem for PHOTOS, TAUOLA, MC-TESTER, ...

This Is Physics Not F77: we need to go through variants for C++ solutions.

This Is Physics Not F77: we need to go through variants for C++ solutions.

Example of pythia 8.1 $Z \to \tau^+\tau^-\gamma$ event

	Barcode	PDG ID	(Px,	Py,	Pz,	E)	Stat	DecayVt
	.							
	.							
	GenVertex:	-11	ID:	0 (X,cT):0				
$Z \to Z$	I: 1	8	23	-1.80e-03,+2.96e-02	-8.11e+01,+1.19e+02		-44	-1
	O: 1	12	23	-1.36e-03,+2.77e-02	-8.11e+01,+1.19e+02		-44	-1
	.							
	.							
	GenVertex:	-13	ID:	0 (X,cT):0				
$Z \to \tau^+\tau^-$	I: 1	12	23	-1.36e-03,+2.77e-02,-8.11e+01,+1.19e+02			-44	-1
	O: 2	15	15	-1.97e+01,-3.85e+01,-3.68e+01,+5.69e+01			-23	-1
		16	-15	+1.97e+01,+3.86e+01,-4.43e+01,+6.20e+01			-23	-1
	GenVertex:	-14	ID:	0 (X,cT):0				
$\tau^+ \to \tau^+ \gamma$	I: 1	16	-15	+1.97e+01,+3.86e+01,-4.43e+01,+6.20e+01			-23	-1
	O: 2	17	-15	+1.71e+01,+3.53e+01,-3.93e+01,+5.56e+01			1	
		18	22	+2.59e+00,+3.15e+00,-5.06e+00,+6.50e+00			1	
	GenVertex:	-15	ID:	0 (X,cT):0				
$\tau^- \to \tau^-$	I: 1	15	15	-1.97e+01,-3.85e+01	-3.68e+01,+5.69e+01		-23	-1
	O: 1	19	15	-1.97e+01,-3.85e+01	-3.67e+01,+5.68e+01		1	

vertex with decay to self & energy-momentum not conserved!

placement of photon in event record

Analytic benchmark

- One of the necessary steps was to verify, that once PHOTOS activated, the lepton spectra will be reproduced as far as the LL corrections to required order.
- Formal solution of QED evolution equation can be written as:

$$D(x,\beta_{ch}) = \delta(1-x)+\beta_{ch}P(x)+\frac{1}{2!}\beta_{ch}^2\{P\times P\}(x)+\frac{1}{3!}\beta_{ch}^3\{P\times P\times P\}(x)+\ldots \quad (10)$$

  where $P(x) = \delta(1-x)(\ln\varepsilon + 3/4) + \Theta(1-x-\varepsilon)\frac{1}{x}(1+x^2)/(1-x)$
  and $\{P\times P\}(x) = \int_0^1 dx_1 \int_0^1 dx_2 \delta(x-x_1x_2)P(x_1)P(x_2)$.
- In the LL contributing regions, phase space Jacobian's of PHOTOS trivialize (CPC 1994). The solution above is reproduced by PHOTOS in a straightforward manner, for each of the outcoming charged lines.
- But it is only a limit! **PHOTOS treat phase space exactly and covers all corners.**

- In a similar way (simplifying phase space Jacobians and droping parts of ME) one can get convinced that distribution of soft photons is as should be for exlusive exponentiation.

- So far we were discussing building blocks, but how does it work in practice?

- Avalanche of numerical results...

- **Important:** We could see that kernel simplified with respect to NLO is sufficient for sub-permille precision. $\longrightarrow$ Much easier to use.

- MC-TESTER by P. Golonka, N. Davidson, T. Przedzinski, Z. Was is used for tests. Idea is to generate histograms of all possible invariant masses which can be constructed from final state momenta.

- One can select events, for example only photons of energy above 1 GeV will be considered as final state.

- On one frame distribution from two program is printed (in logarithmic scale) and their ration (in linear scale).

- No of events of distinct (in the selected way) final states is printed too.

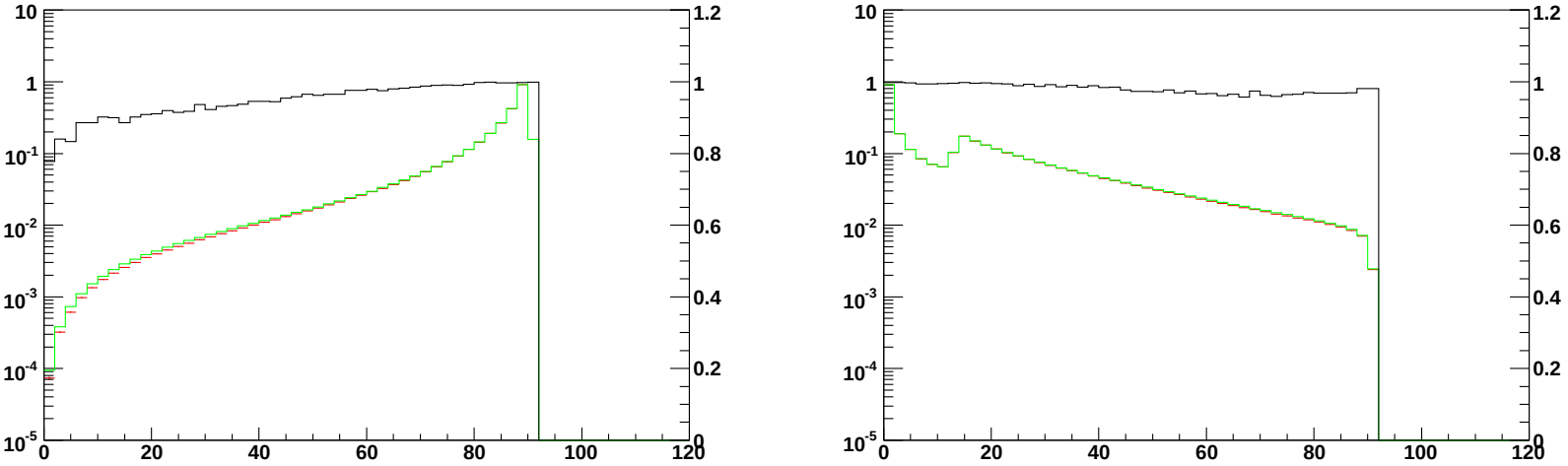

Figure 1: Comparison of standard PHOTOS and KORALZ for single photon emission. In the left frame the invariant mass of the $\mu^+\mu^-$ pair; SDP=0.00534. In the right frame the invariant mass of $\mu^-\gamma$; SDP=0.00296. The histograms produced by the two programs (logarithmic scale) and their ratio (linear scale, black line) are plotted in both frames. The fraction of events with hard photon was 17.4863 ± 0.0042% for KORALZ and 17.6378 ± 0.0042% for PHOTOS.

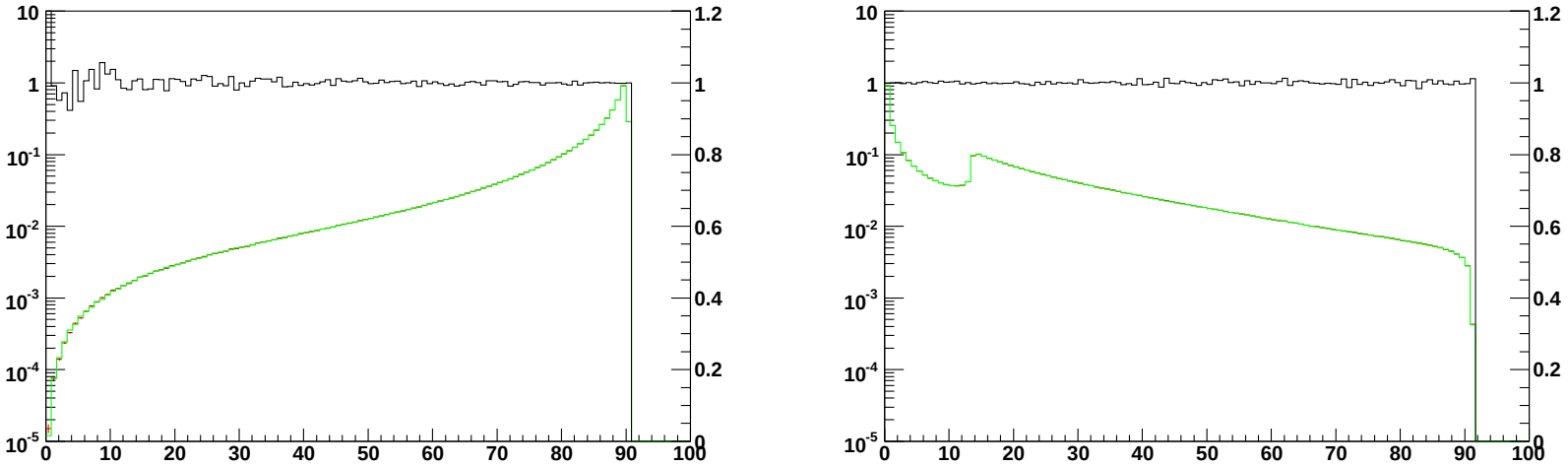

Figure 2: Comparisons of improved PHOTOS and KORALZ for single photon emission. In the left frame the invariant mass of the $\mu^+\mu^-$ pair. In the right frame the invariant mass of $\mu^-\gamma$ pair is shown. In both cases differences between PHOTOS and KORALZ are below statistical error. The fraction of events with hard photon was 17.4890 $\pm$ 0.0042% for KORALZ and 17.4926 $\pm$ 0.0042% for PHOTOS.

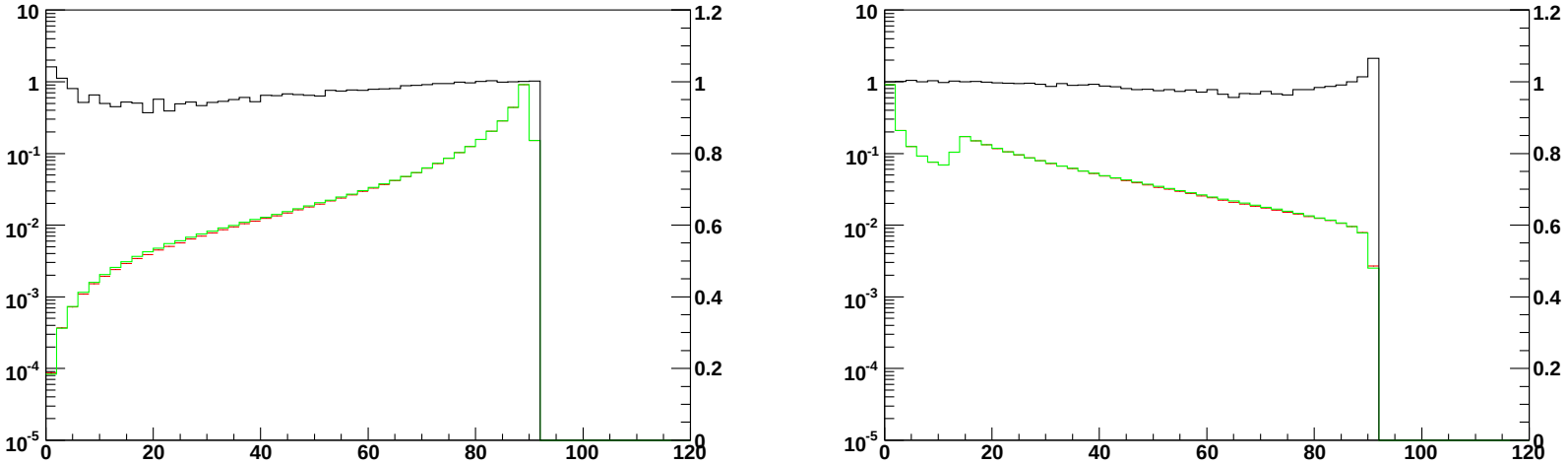

Figure 3: Comparison of standard PHOTOS with multiple photon emission and KKMC with second order matrix element and exponentiation. In the left frame the invariant mass of the $\mu^+\mu^-$ pair; SDP=0.00409. In right frame the invariant mass of the $\mu^-\gamma$ pair; SDP=0.0025. The pattern of differences between PHOTOS and KKMC is similar to the one of Fig 1. The fraction of events with hard photon was 16.0824 $\pm$ 0.0040% for KKMC and 16.1628 $\pm$ 0.0040% for PHOTOS.

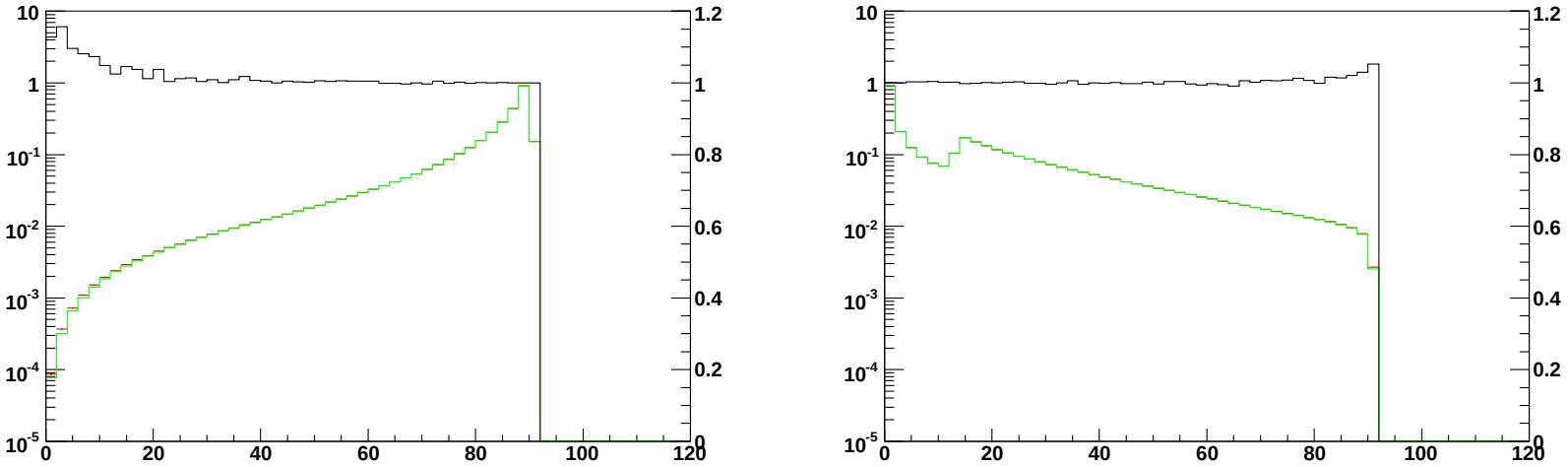

Figure 4: Comparisons of improved PHOTOS with multiple photon emission and KKMC with second order matrix element and exponentiation. In the left frame the invariant mass of the $\mu^+\mu^-$ pair; SDP=0.0000249. In the right frame the invariant mass of the $\mu^-\gamma$ pair; SDP=0.0000203. The fraction of events with hard photon was 16.0824 $\pm$ 0.004% for KKMC and 16.0688 $\pm$ 0.004% for PHOTOS.

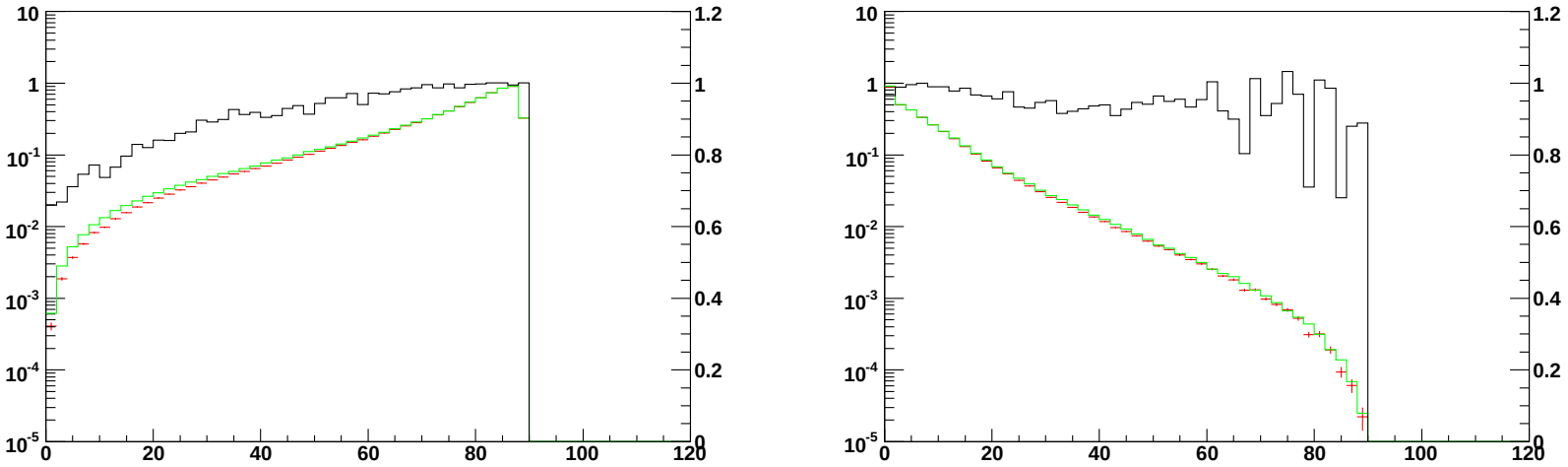

Figure 5: Comparisons of standard PHOTOS with multiple photon emission and KKMC with second order matrix element and exponentiation. In the left frame the invariant mass of the $\mu^+\mu^-$ pair; SDP= 0.00918. In the right frame the invariant mass of the $\gamma\gamma$ pair; SDP=0.00268. The fraction of events with two hard photons was $1.2659 \pm 0.0011\%$ for KKMC and $1.2952 \pm 0.0011\%$ for PHOTOS.

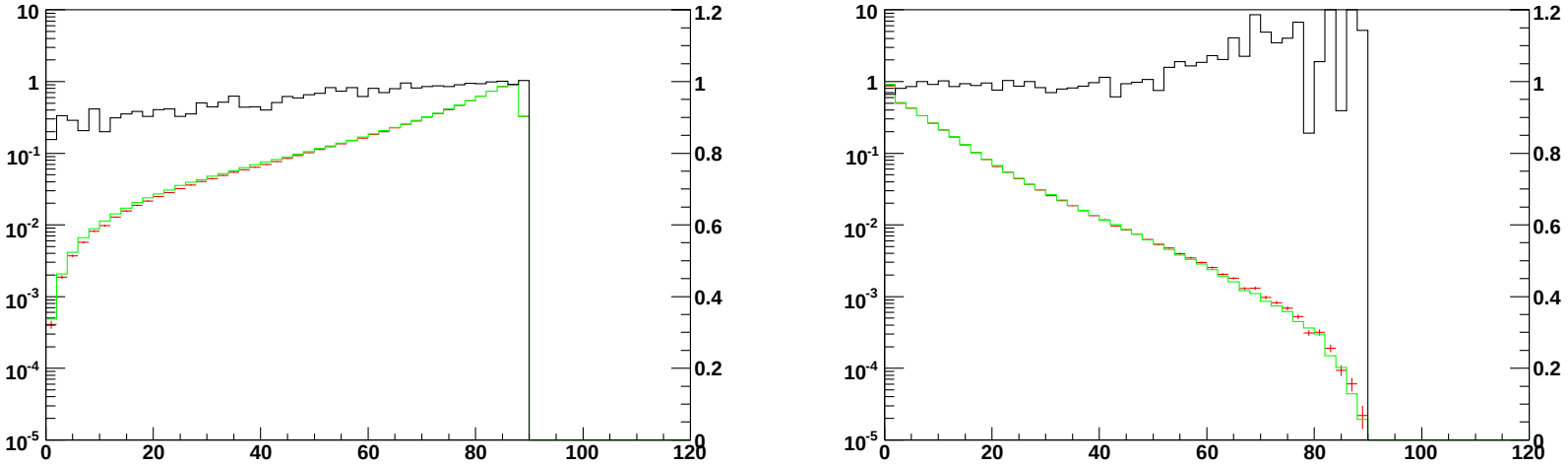

Figure 6: Comparisons of improved PHOTOS with multiple photon emission and KKMC with second order matrix element and exponentiation. In the left frame the invariant mass of the $\mu^+\mu^-$ *pair; SDP= 0.00142. In the right frame the invariant mass of the* $\gamma\gamma$*; SDP=0.00293. The fraction of events with two hard photons was 1.2659* $\pm$ *0.0011% for KKMC and 1.2868* $\pm$ *0.0011% for PHOTOS.*

Matrix Element for Z decay:

- Our discussion of double emission amplitudes was started from the single photon one
- The same is true for amplitudes of other processes. We have to check if they are similar to this for Z decay.
- In particular only if they structure match we can expect that our discussion of multiemission may apply as well.
- $$I = I^A + I^B + I^C$$
- $$I = \not{J}\left[\left(\frac{p\cdot e_1}{p\cdot k_1} - \frac{q\cdot e_1}{q\cdot k_1}\right)\right] - \left[\frac{1}{2}\frac{\not{e}_1\not{k}_1}{p\cdot k_1}\right]\not{J} + \not{J}\left[\frac{1}{2}\frac{\not{e}_1\not{k}_1}{q\cdot k_1}\right]$$

three gauge invariant parts, I^A is eikonal; I^B, I^C carry collinear contrib from p and q

Scalar QED: $B \to K\pi$ decays – pure I^A

- The one-loop QED correction to the decay width can be represented as the sum o f the Born contribution with the contributions due to virtual loop diagrams and soft and hard photon emissions.

$$d\Gamma^{\rm Total} = d\Gamma^{\rm Born}\left\{1+\frac{\alpha}{\pi}\left[\delta^{\rm Soft}(m_\gamma,\omega)+\delta^{\rm Virt}(m_\gamma,\mu_{UV})\right]\right\} + d\Gamma^{\rm Hard}(\omega)$$

- where for **Neutral meson decay channels**, hard photon contribution:

$$d\Gamma^{\rm Hard} = |A^{\rm Born}|^2 4\pi\alpha\left(q_1\frac{k_1.\epsilon}{k_1.k_\gamma}-q_2\frac{k_2.\epsilon}{k_2.k_\gamma}\right)^2 dLips_3(P\to k_1,k_2,k_\gamma)$$

- for **Charged meson decay channels**, hard photon contribution:

$$d\Gamma^{\rm Hard} = |A^{\rm Born}|^2 4\pi\alpha\left(q_1\frac{k_1.\epsilon}{k_1.k_\gamma}-q\frac{P.\epsilon}{P.k_\gamma}\right)^2 dLips_3(P\to k_1,k_2,k_\gamma)$$

Scalar QED for $\gamma^* \to \pi^+\pi^-\gamma$: I^A and non-leading

- This case is different, because of spin structure. One can not make spin of initial state out of internal spin of outgoing particles.

$$H^\mu = \frac{e^2 F_{2\pi}(p^2)}{p^2}\left\{(q_1+k-q_2)^\mu \frac{q_1\cdot\epsilon^*}{q_1\cdot k} + (q_2+k-q_1)^\mu \frac{q_2\cdot\epsilon^*}{q_2\cdot k} - 2\epsilon^{*\mu}\right\}$$

- As in case of Z decay one can separate spin amplitude into gauge invariant parts ($C = \frac{e^2 F_{2\pi}(p^2)}{p^2}$):

$$H^\mu_I = C\,(q_1-q_2)^\mu\left(\frac{q_1\cdot\epsilon^*}{q_1\cdot k} - \frac{q_2\cdot\epsilon^*}{q_2\cdot k}\right), H^\mu_{II} = C\,\left(k^\mu\left(\frac{q_1\cdot\epsilon^*}{q_1\cdot k} + \frac{q_2\cdot\epsilon^*}{q_2\cdot k}\right) - 2\epsilon^{*\mu}\right), \tag{11}$$

- This can be improved with the following change:

$$H^\mu_{I'} = C\,\left((q_1-q_2)^\mu + k^\mu\frac{q_2\cdot k - q_1\cdot k}{q_2\cdot k + q_1\cdot k}\right)\left(\frac{q_1\cdot\epsilon^*}{q_1\cdot k} - \frac{q_2\cdot\epsilon^*}{q_2\cdot k}\right), \tag{12}$$

$$H^\mu_{II'} = C\,\left(\frac{k^\mu}{q_2\cdot k + q_1\cdot k}(q_1\cdot\epsilon^* + q_2\cdot\epsilon^*) - \epsilon^{*\mu}\right). \tag{13}$$

- In the second case non-eikonal term is free of collinear logarithm, but is non trivial and contributes 0.2 % to total rate, thus can be numerically studied!

QED for $W \to l\nu_l\gamma$: I^A, I^B and non-leading

$$
\begin{aligned}
M^{\sigma}_{\lambda,\lambda_\nu,\lambda_l}(k,Q,p_\nu,p_l) \;=\; & \left[\frac{Q_l}{2\,k\cdot p_l}b_\sigma(k,p_l) - \frac{Q_W}{2\,k\cdot Q}\left(b_\sigma(k,p_l)+b_\sigma(k,p_\nu)\right)\right] B^{\lambda}_{\lambda_l,\lambda_\nu}(p_l,Q,p_\nu) \\
& + \frac{Q_l}{2\,k\cdot p_l}\sum_{\rho=\pm} U^{\sigma}_{\lambda_l,\rho}(p_l,m_l,k,0,k,0)B^{\lambda}_{\rho,-\lambda_\nu}(k,Q,p_\nu) \\
& - \frac{Q_W}{2\,k\cdot Q}\sum_{\rho=\pm}\Big(B^{\lambda}_{\lambda_l,-\rho}(p_l,Q,k)U^{\sigma}_{-\rho,-\lambda_\nu}(k,0,k,0,p_\nu,0) \\
& \qquad + U^{\sigma}_{\lambda_l,\rho}(p_l,m_l,k,0,k,0)B^{\lambda}_{\rho,-\lambda_\nu}(k,Q,p_\nu)\Big)\,,
\end{aligned}
\tag{14}
$$

$$
\begin{aligned}
B^{\lambda}_{\lambda_1,\lambda_2}(p_1,Q,p_2) &\equiv \frac{g}{2\sqrt{2}}\bar{u}(p_1,\lambda_1)\,\widehat{\epsilon}^{\lambda}_{W}(Q)(1+\gamma_5)\,v(p_2,\lambda_2)\,, \\
U^{\sigma}_{\lambda_1,\lambda_2}(p_1,m_1,k,0,p_2,m_2) &\equiv \bar{u}(p_1,\lambda_1)\,\widehat{\epsilon}^{\sigma}_{\gamma}(k)\,u(p_2,\lambda_2)\,, \\
\delta_{\lambda_1\lambda_2}b_\sigma(k,p) &\equiv U^{\sigma}_{\lambda_1,\lambda_2}(p,m,k,0,p,m)\,,
\end{aligned}
\tag{15}
$$

Q_l and Q_W are the electric charges of the fermion l and the W boson, respectively, in units of the positron charge, $\epsilon^{\sigma}_{\gamma}(k)$ and $\epsilon^{\lambda}_{W}(Q)$ denote respectively the polarization vectors of the photon and the W boson. An expression of the function $U^{\sigma}_{\lambda_1,\lambda_2}$ in terms of the massels spinors.

Matrix Element (anything useful seen?):

- We have seen that in all cases terms I^A, I^B, I^C appear
- These are the only ones which carry soft or collinear contributions
- That is why universal weight of Photos could be defined.
- That is also why the soultion defined from Z amplitudes work for other processes as well
- part of NLO proof.
- Tests confirm that NLO complete kernel (process dependent) is not necessary even for sub-permille precision level $\longrightarrow$ good for users.

$B^- \to \pi^0 K^-$: *standard PHOTOS* looks good, but ...

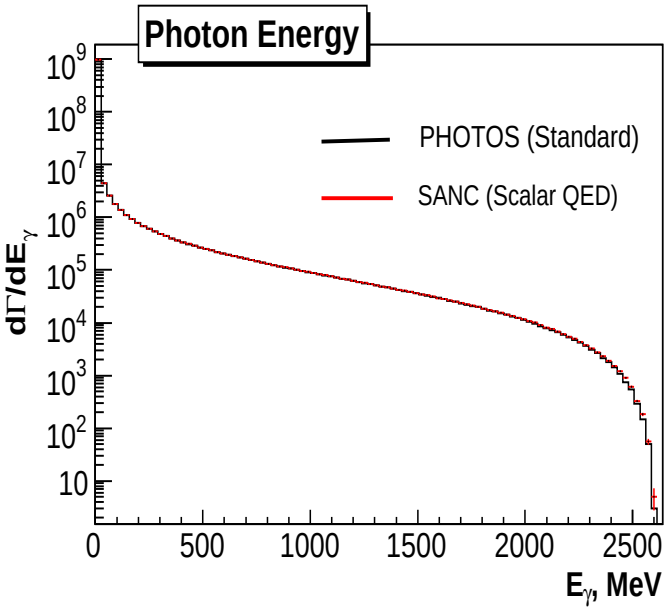

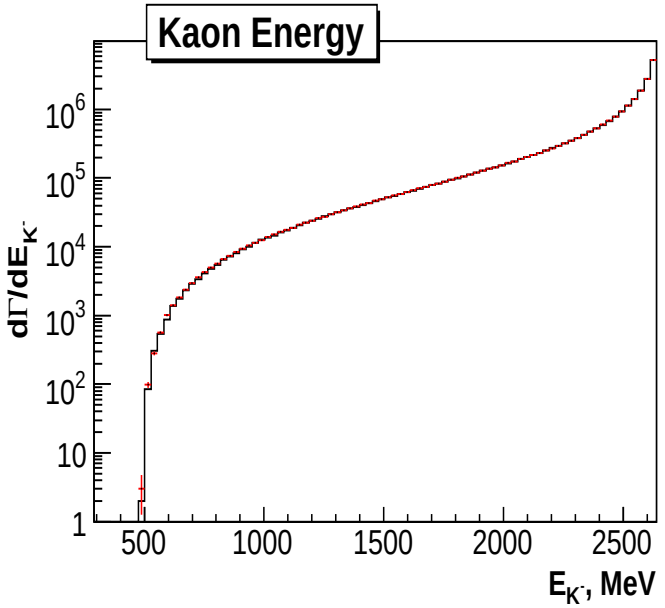

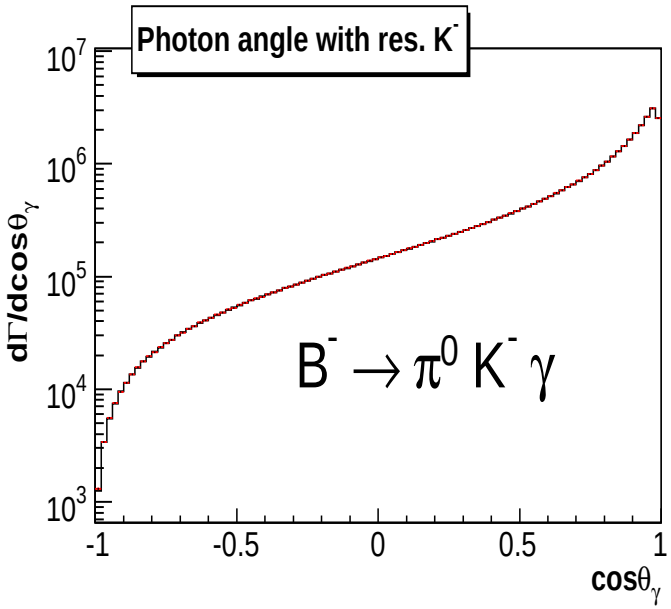

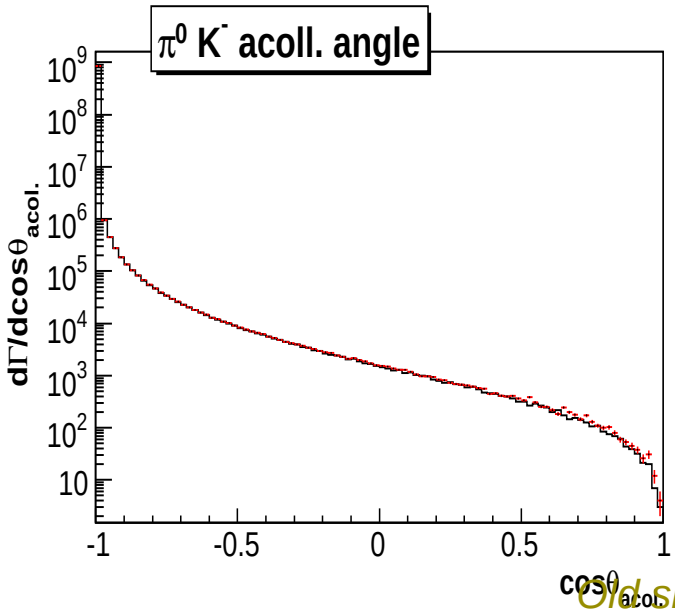

$B^- \to \pi^0 K^-$: standard PHOTOS not perfect

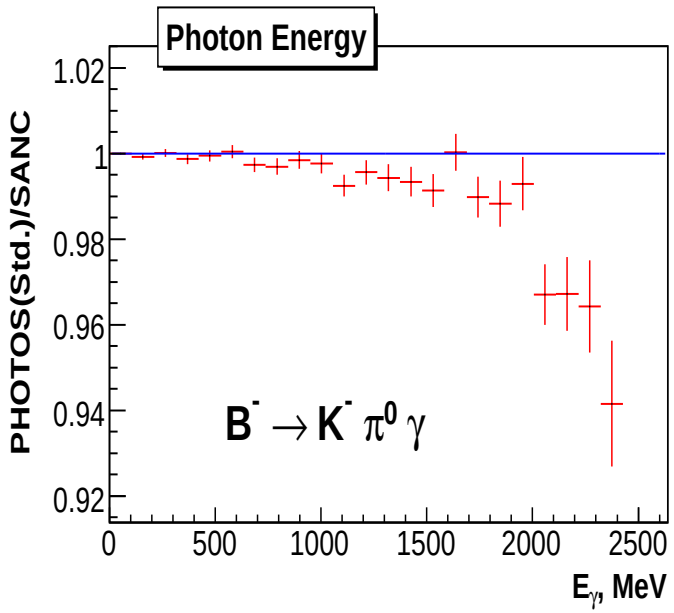

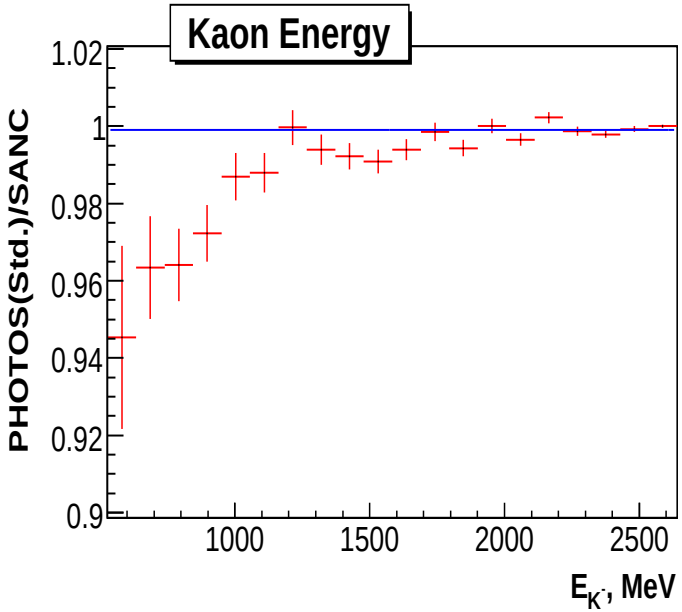

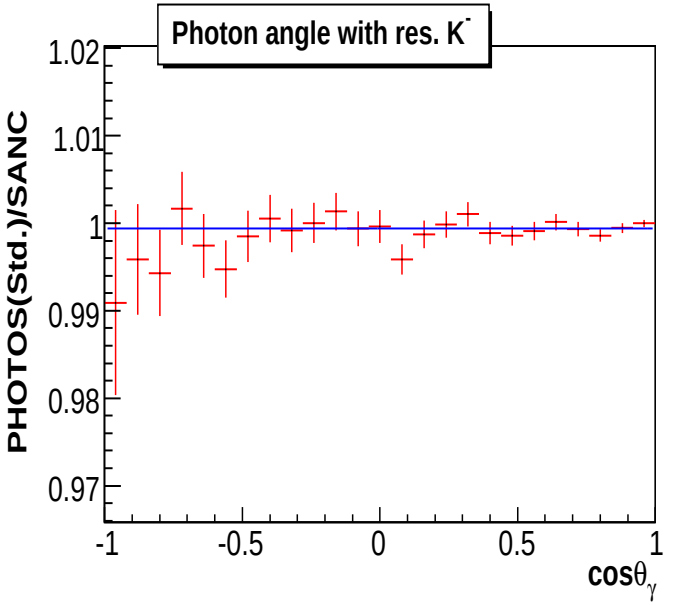

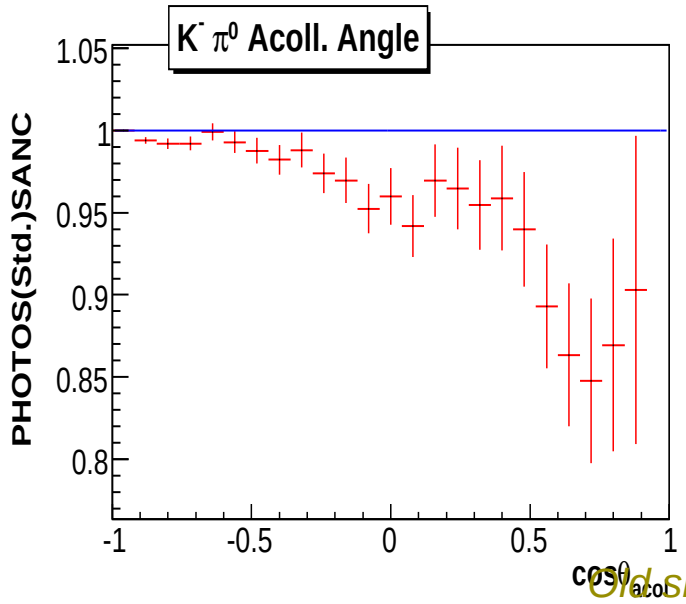

$B^- \to \pi^0 K^-$: NLO improved PHOTOS Looks good

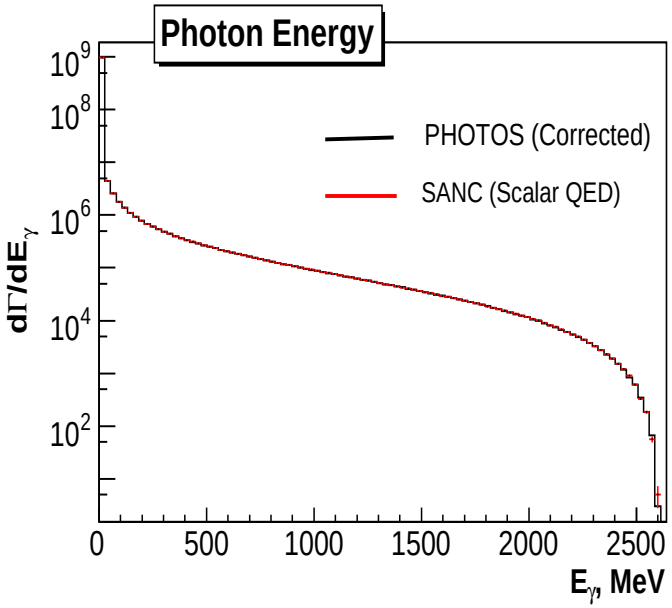

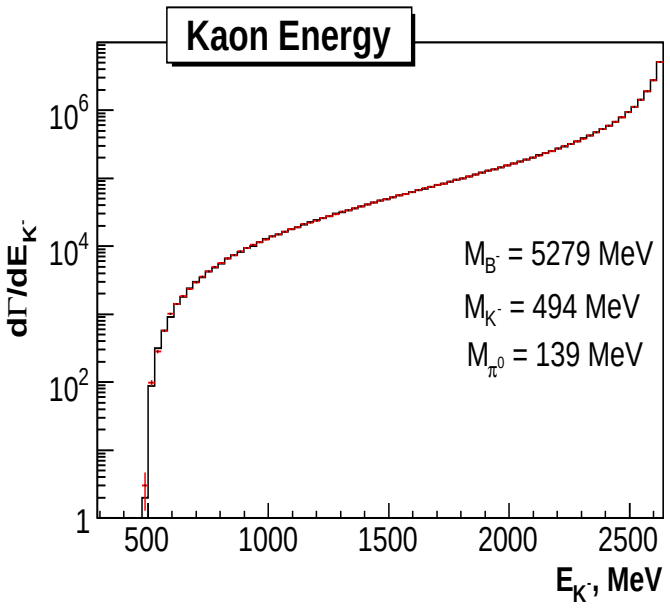

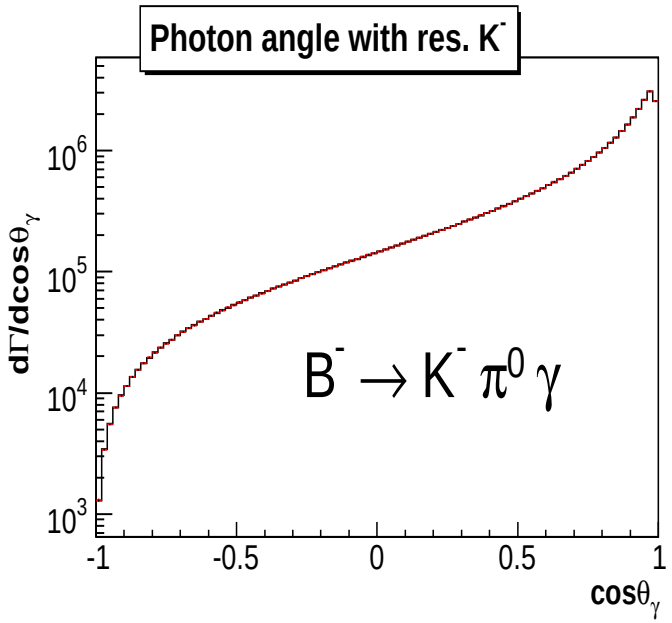

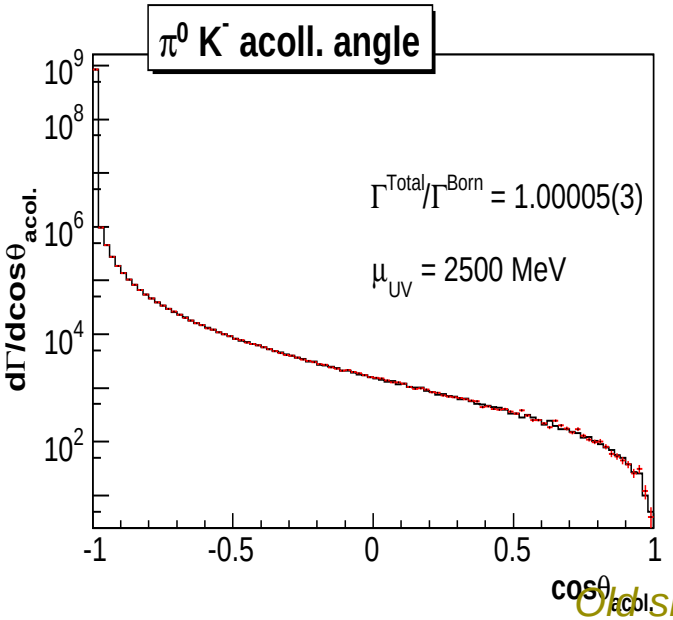

$B^- \to \pi^0 K^-$: NLO improved PHOTOS ... and is good.

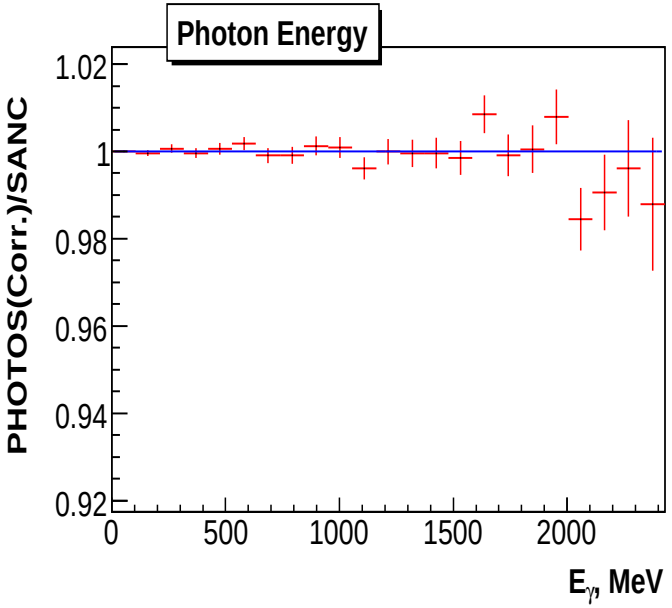

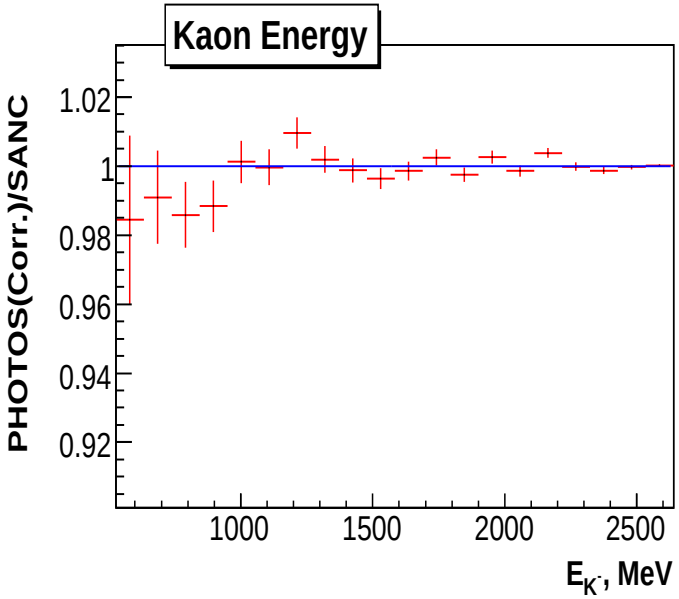

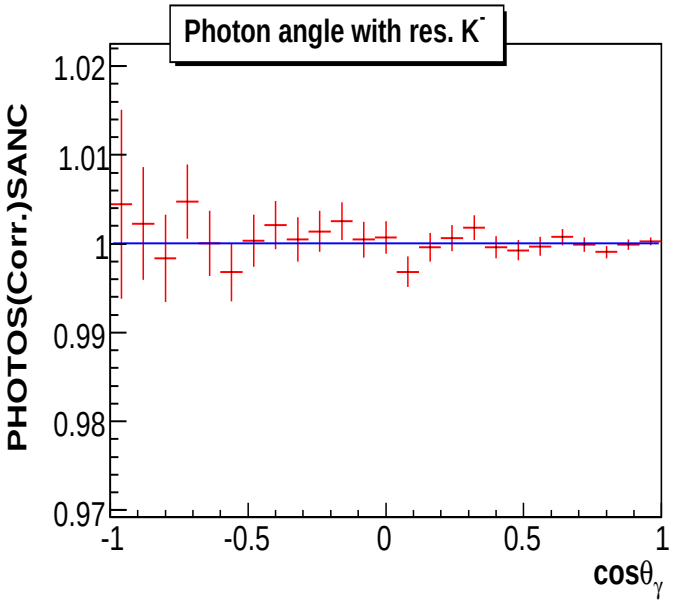

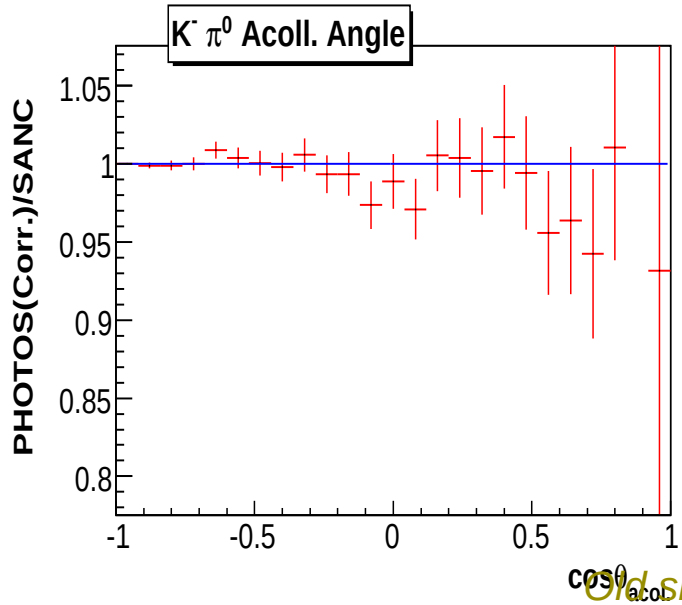

$B^0 \to \pi^- K^+$: standard PHOTOS Looks good ...

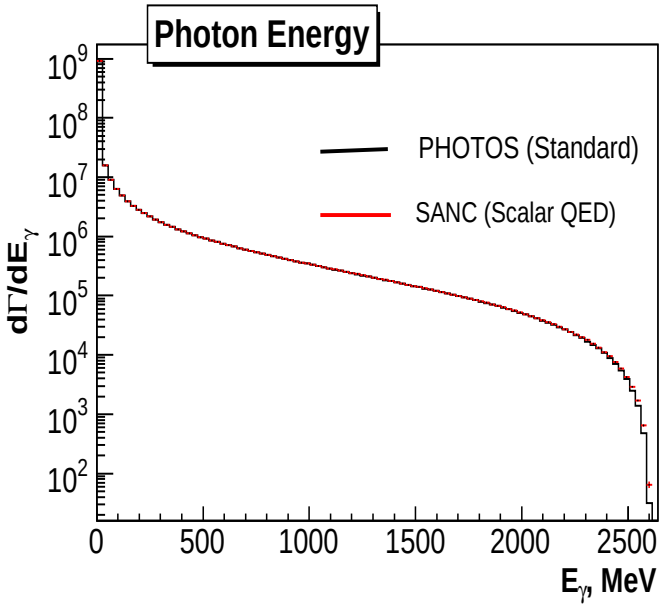

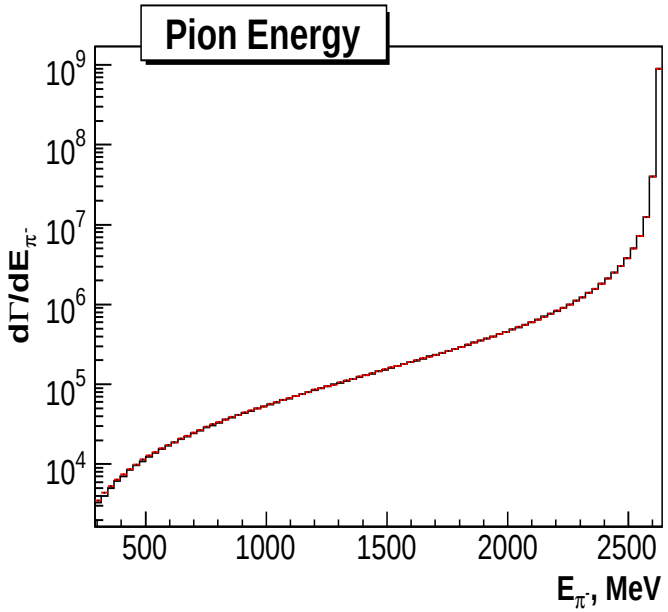

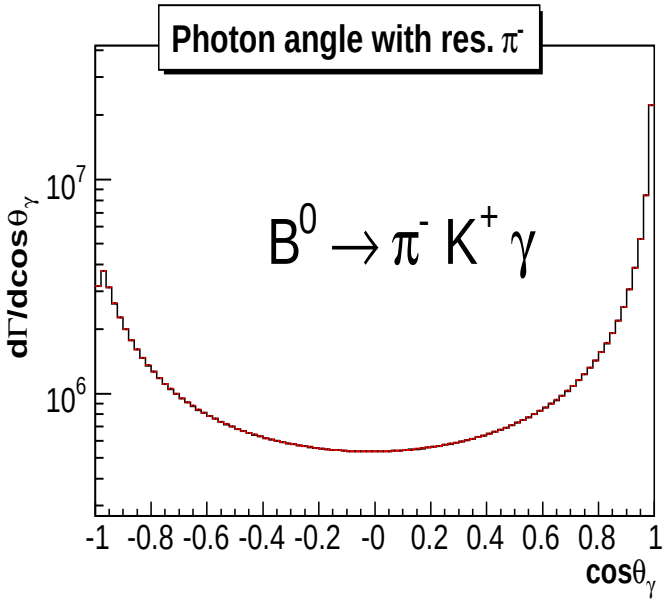

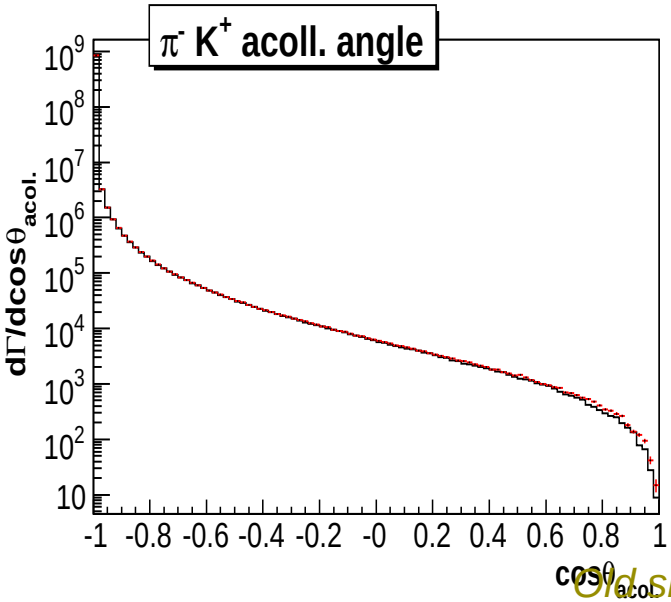

$B^0 \to \pi^- K^+$: standard PHOTOS ... but not perfect.

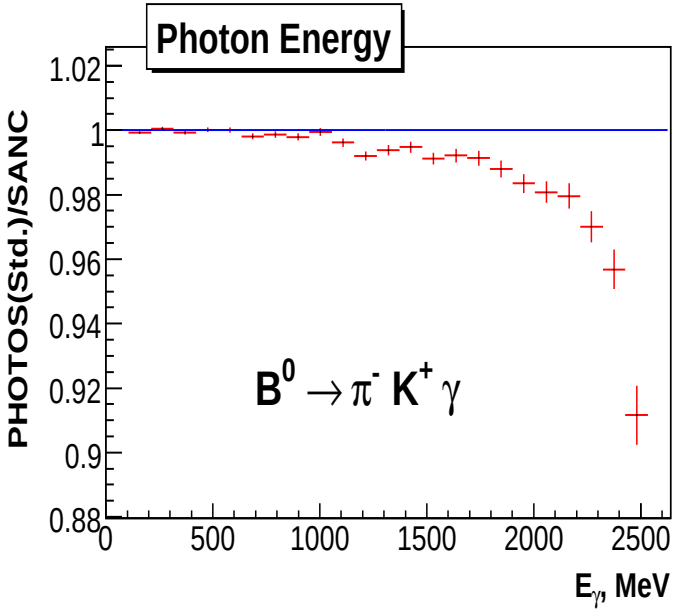

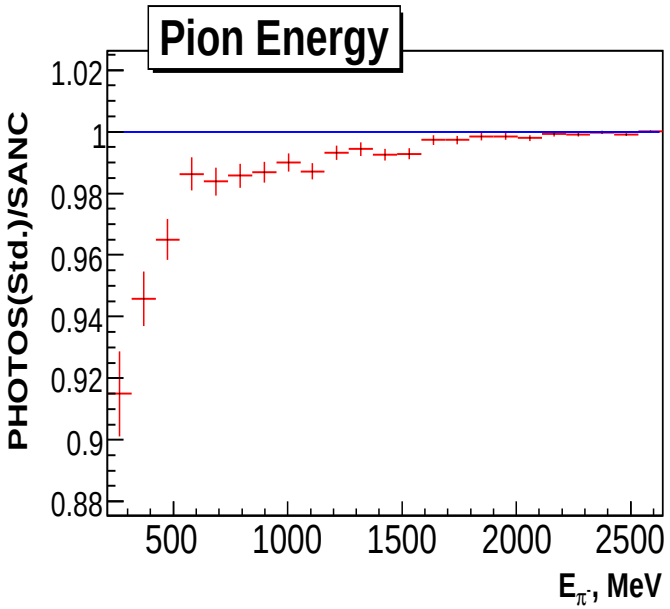

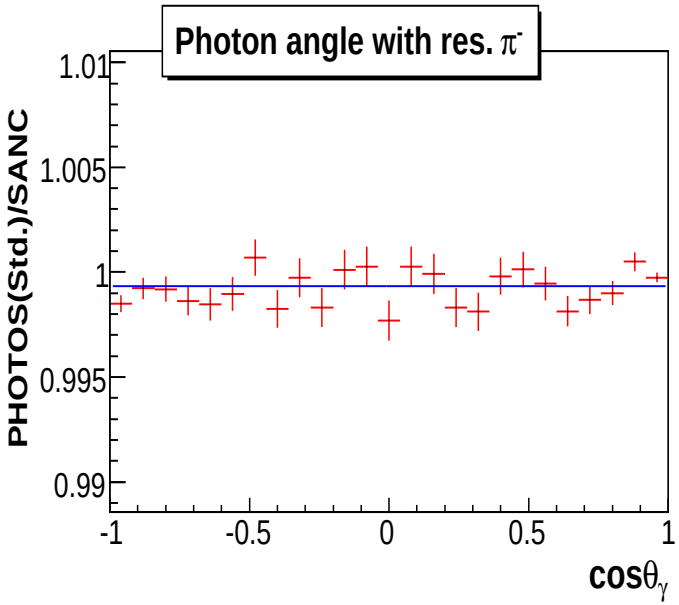

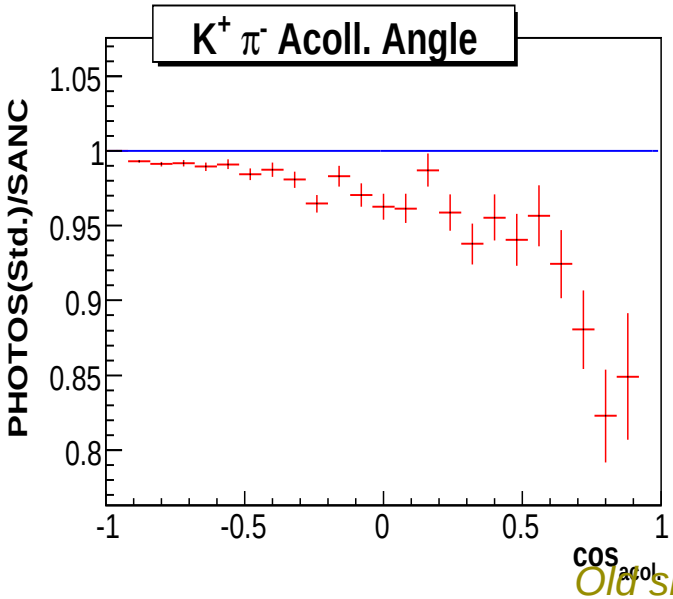

$B^0 \to \pi^- K^+$: NLO improved PHOTOS Looks good ...

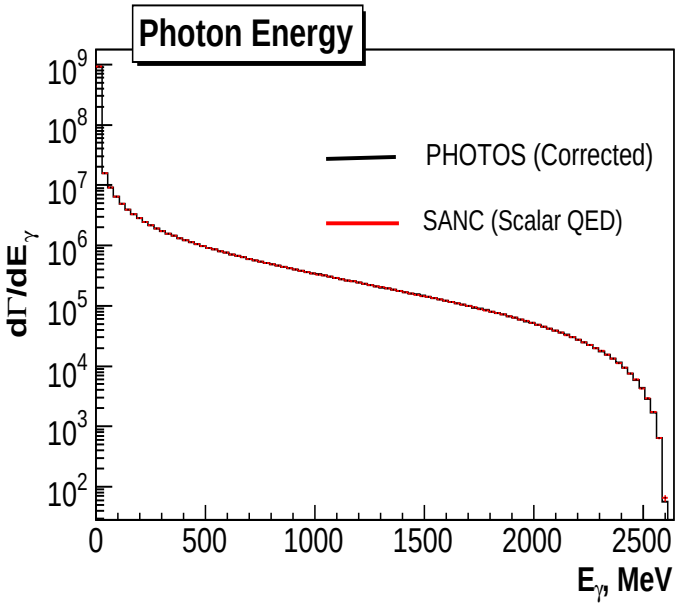

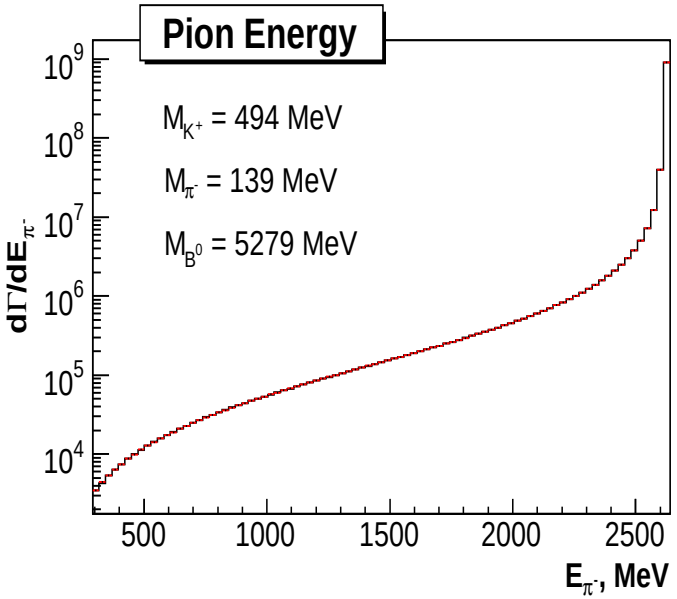

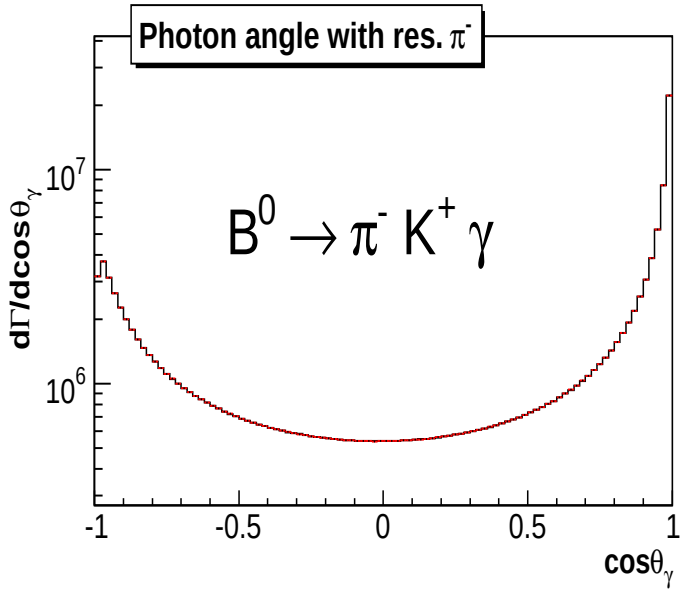

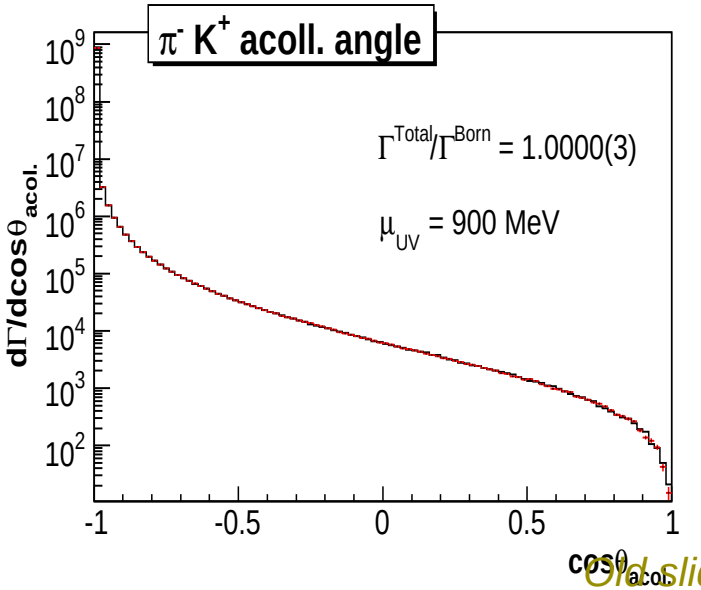

$B^0 \to \pi^- K^+$; NLO improved PHOTOS ... also perfect !

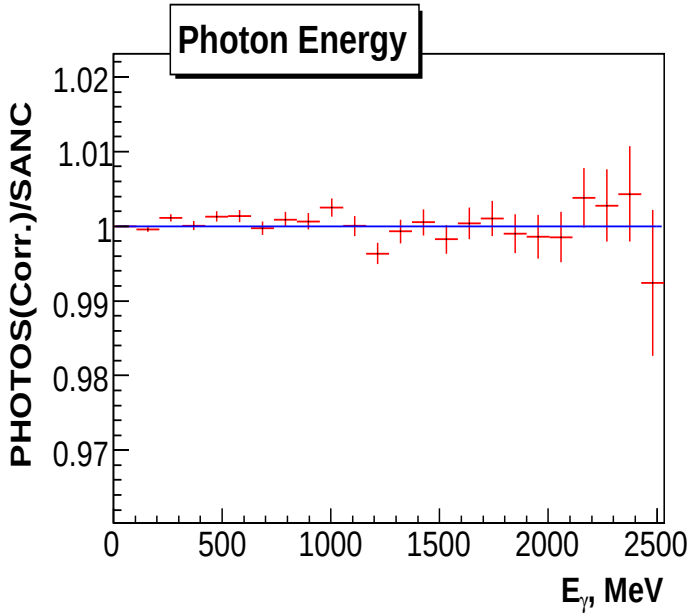

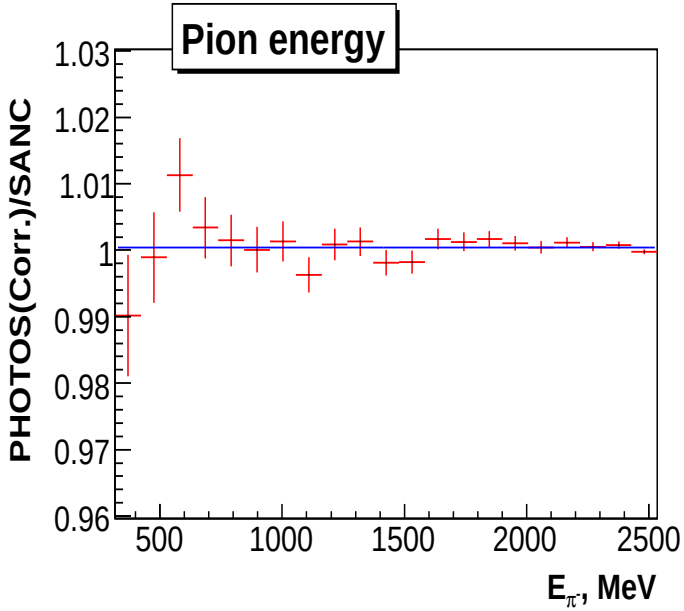

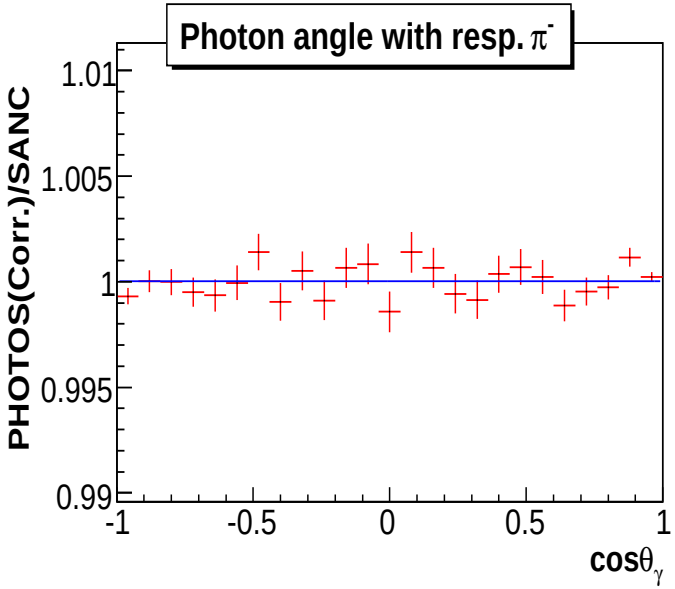

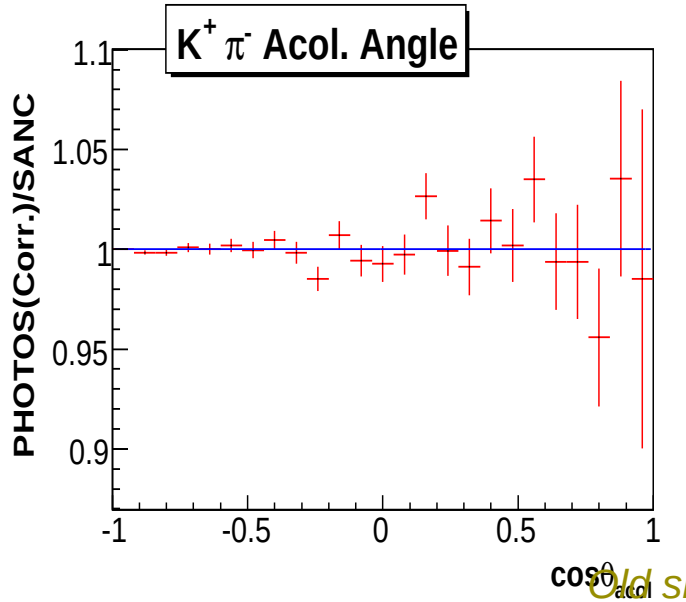

Other processes

Results for W, H, and $\gamma^* \to \pi^+\pi^-$ are of similar quality.

Tests for $K^\pm \to l^\pm\nu\pi^+\pi^-$ are going on. In general for more than two body decays effort of tests was never matching the one presented earlier.

$\tau \to l\nu\bar{\nu}(\gamma)$ PHOTOS vs TAUOLA

Plot of worst agreement for the channel. Distribution of $\gamma\nu_\tau\nu_\mu$ system mass is shown .

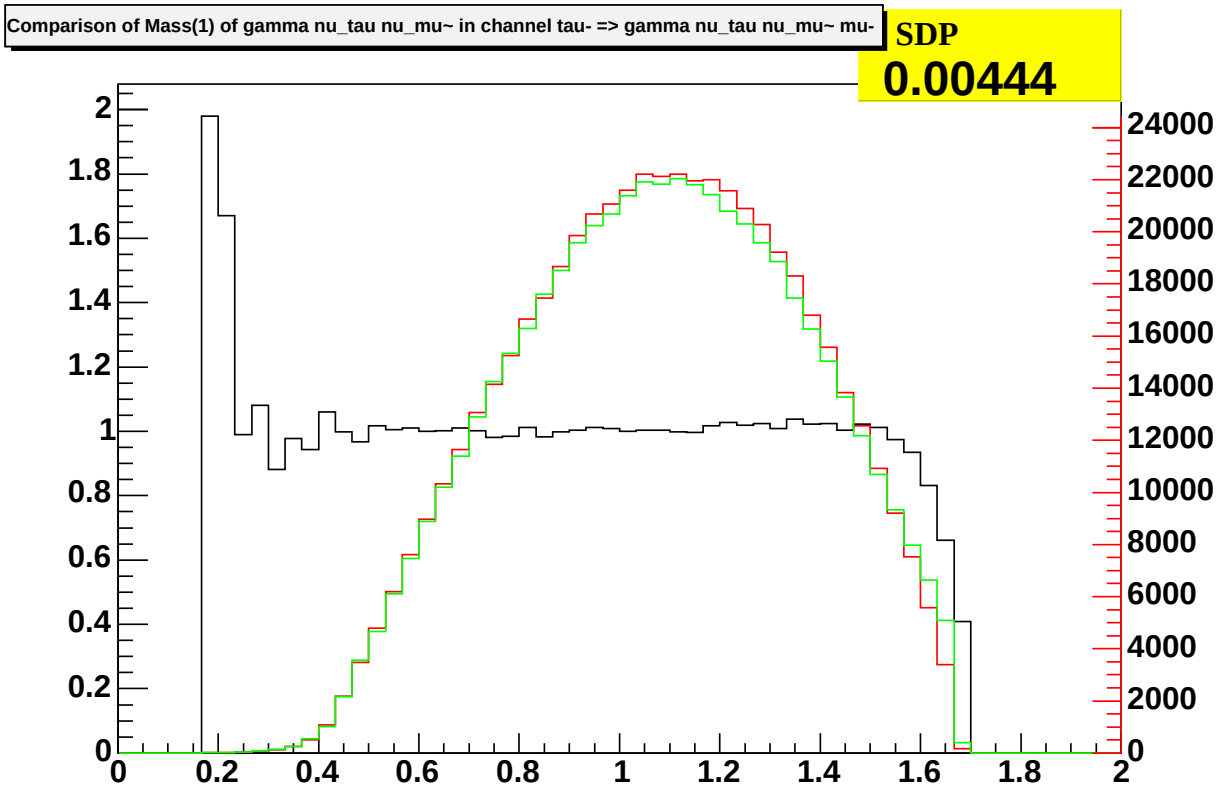

Also the fraction of events with photon above threshold agrees better than permille level.

In TAUOLA complete matrix element, comparison test PHOTOS approximations and design.

Phys. Lett, B 303 (1993) 163-169

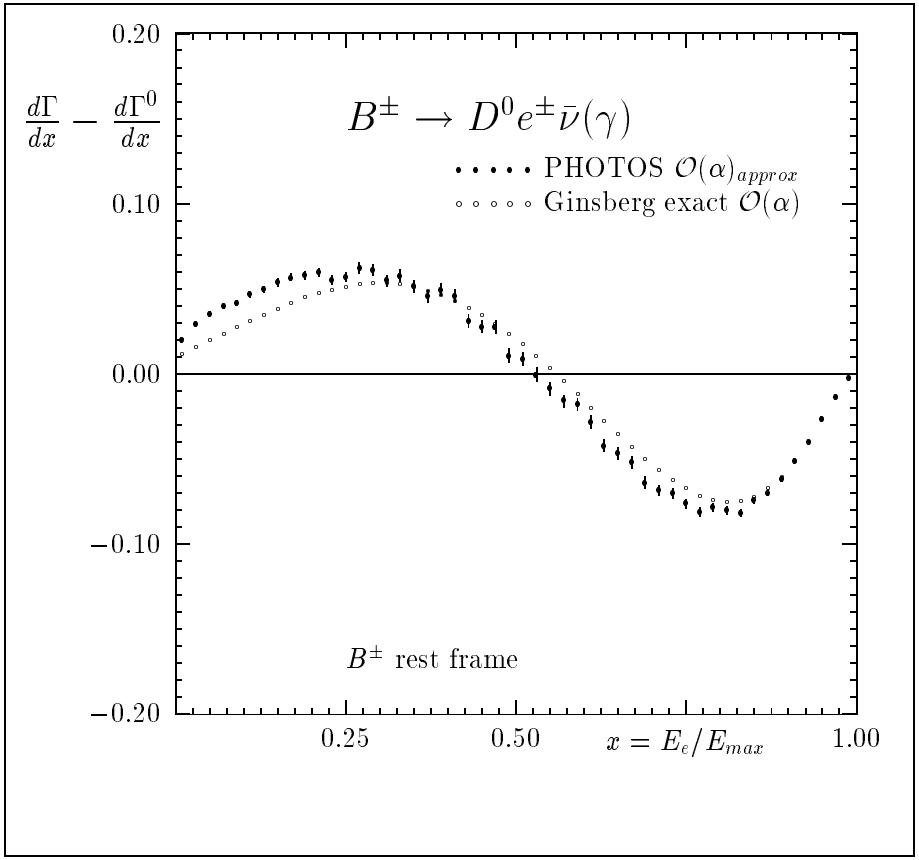

Radiative correction to the decay rate $(d\Gamma/dx - d\Gamma^0/dx)$ for $B^{\pm} \to D^0 e^{\pm} \bar{\nu}(\gamma)$ in the $B^{\pm}$ rest frame. Open circles are from the exact analytical formula [2], points with the marked statistical errors from PHOTOS applied to JETSET 7.3. A total of 10^7 events have been generated. The results are given in units of $(G_{\mu}^2 m_B^5/32\pi^3) N_{\eta} |V_{cb}|^2 |f_+^D|^2$, where $N_{\eta} = \eta^5 \int_0^1 x^2(1-x)^2/(1-\eta x)dx$ and $\eta = 1 - m_D^2/m_B^2$.

- *"QED bremsstrahlung in semileptonic B and leptonic τ decays"* by E. Richter-Was.
- agreement up to 1%
- disagreement in the low-x region due to missing sub-leading terms
- study performed in 1993.

$K \to \pi e \nu(\gamma)$ PHOTOS w/Interf vs Gasser

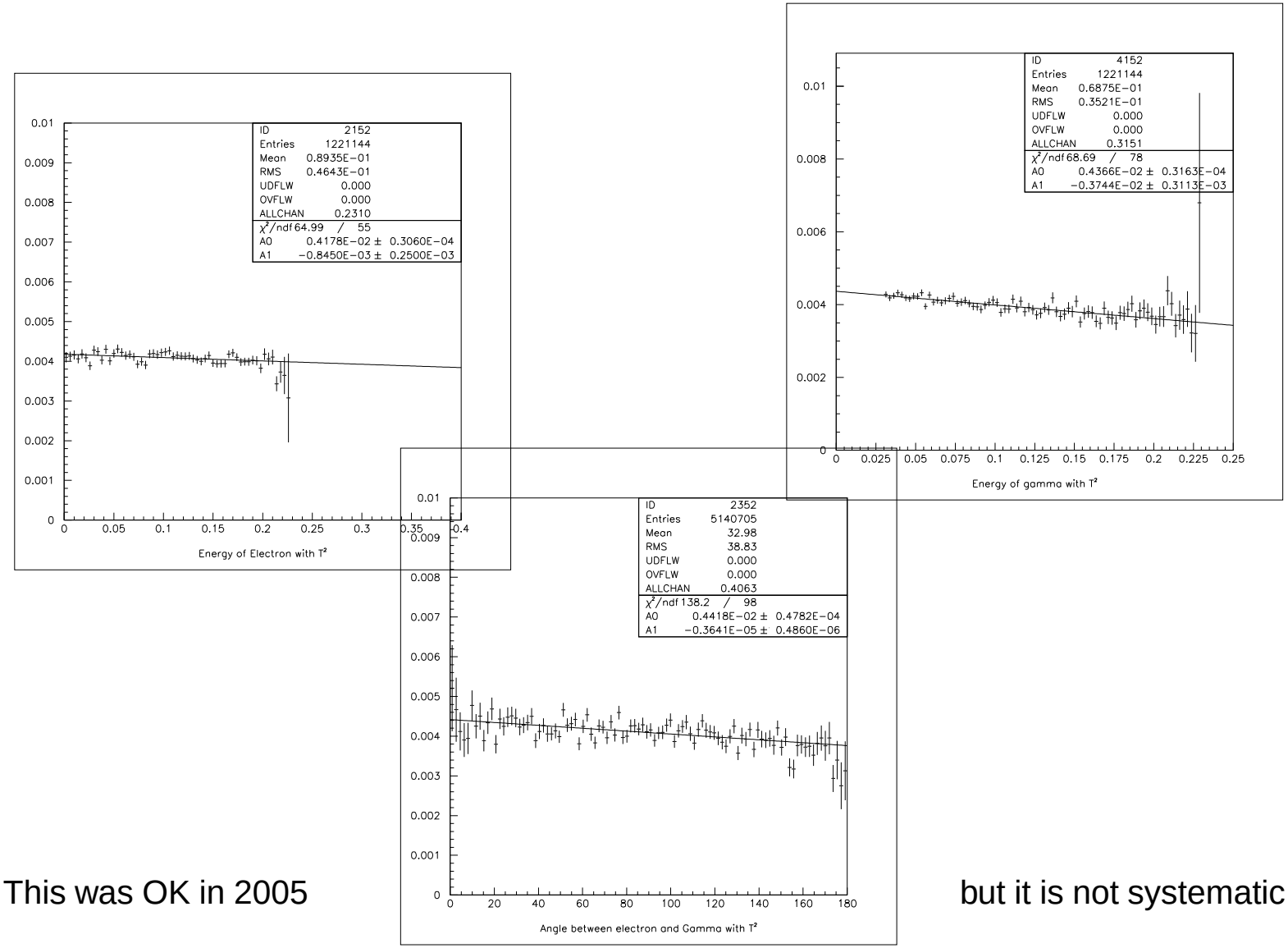

This was OK in 2005

but it is not systematic work.

Events with and without photon:

$R = \frac{\Gamma_{K_{e3\gamma}}}{\Gamma_{K_{e3}}}$	PHOTOS %	GASSER %
$5 < E_\gamma < 15\, MeV$	2.38	2.42
$15 < E_\gamma < 45\, MeV$	2.03	2.07
$\Theta_{e,\gamma} > 20$	0.876	0.96

courtesy of NA48 and Prof. L.Litov

This results can be obtained starting from PHOTOS version 2.13.

Summary

● It was a pleasure to give a seminar in NIKHEF. At time we started the project neither Bob nor me were dreaming that it could become so popular and for so long as well! Also precision potential of algorithm was underesimated. **NOW:**

● Program is based on exact multiphoton phase space and matrix element

● For some channels process specific kernels based on exact first order matrix elements were introduced (but are not distributed because their effects are so small).

● Spin amplitudes were essential in program development.

● In construction we rely on properties of factorization and those properties of QED matrix elements which lead to YFS exponentiation. Studies of double emission amplitudes were necessary. For example in paper on $e^+e^- \to \nu_e\bar{\nu}_e\gamma\gamma$, EPJC C44 (2005) 489, input for emissions from fermions and vectors can be found.

● Since couple of years program can be used as precision tool. For most of benchmarks precision tag achieved is below 0.1 %.

● Program works as after-burner. This is advantageous, events generated by other

programs can be modified. It is a challenge too. Numerical stability and correctness of PHOTOS operation depends on quality of events read in.

- Implementation for FORTAN HEPEVT is widely in use. For C++ HepMC at present beta version exist only.

Extra transparencies

Deatails of parametrization used in G and G^{-}

1. we are using **STANDARD and FORMAL** parametrizations of Lorentz group. One can express it with the help of consecutive boosts and rotations.
2. Convenient for Monte Calro event construction!
3. For the definition of coordinate system in the P-rest frame the $\hat{x}$ and $\hat{y}$ axes of the laboratory frame boosted to the rest frame of P can be used. The orthogonal right-handed system can be constructed with their help in a standard way.
4. We choose polar angles θ_1 and ϕ_1 defining the orientation of the four momentum $\bar{k}_2$ in the rest frame of P. In that frame $\bar{k}_1$ and $\bar{k}_2$ are back to back[a], see fig. (7).
5. The previous two points would complete the definition of the two-body phase space, if both $\bar{k}_1$ and $\bar{k}_2$ had no measurable spin degrees of freedom visualizing themselves e.g. through correlations of the secondary decay products' momenta. Otherwise we need to know an additional angle ϕ_X to complete the set of Euler angles defining the relative orientation of the axes of the P rest-frame system with the coordinate system used in the rest-frame of $\bar{k}_2$ (and possibly also of $\bar{k}_1$), see fig. (8).

[a] In the case of phase space construction for multi-body decays $\bar{k}_2$ should read as a state representing the sum of all decay products of P but $\bar{k}_1$.

6. If both rest-frames of $\bar{k}_1$ and $\bar{k}_2$ are of interest, their coordinate systems are oriented with respect to P with the help of θ_1, ϕ_1, ϕ_X. We assume that the coordinate systems of $\bar{k}_1$ and $\bar{k}_2$ are connected by a boost along the $\bar{k}_2$ direction, and in fact share axes: $z' \uparrow\downarrow z''$, $x' \uparrow\uparrow x''$, $y' \uparrow\downarrow y''$.

7. For the three-body phase space: We take the photon energy k_γ in P rest frame. We calculate: photon, k_1 and k_2 energies, all in $k_1 + k_2$ frame.

8. We use the angles θ, ϕ, in the rest-frame of the $k_1 + k_2$ pair: angle θ is an angle between the photon and k_1 direction (i.e. $-z''$). Angle ϕ defines the photon azimuthal angle around z'', with respect to x'' axis (of the k_2 rest-frame), see fig. (9).

9. If all k_1, k_2 and $k_1 + k_2$ rest-frames exist, then the x-axes for the three frames are chosen to coincide. It is OK, all frmes connected by boosts along z'' see fig. (9).

10. To define orientation of k_2 in P rest-frame coordinate system, and to complete construction of the whole event, we will re-use Euler angles of $\bar{k}_2$: ϕ_X, θ_1 and ϕ_1 (see figs. 10 and 11), defined again of course in the rest frame of P.

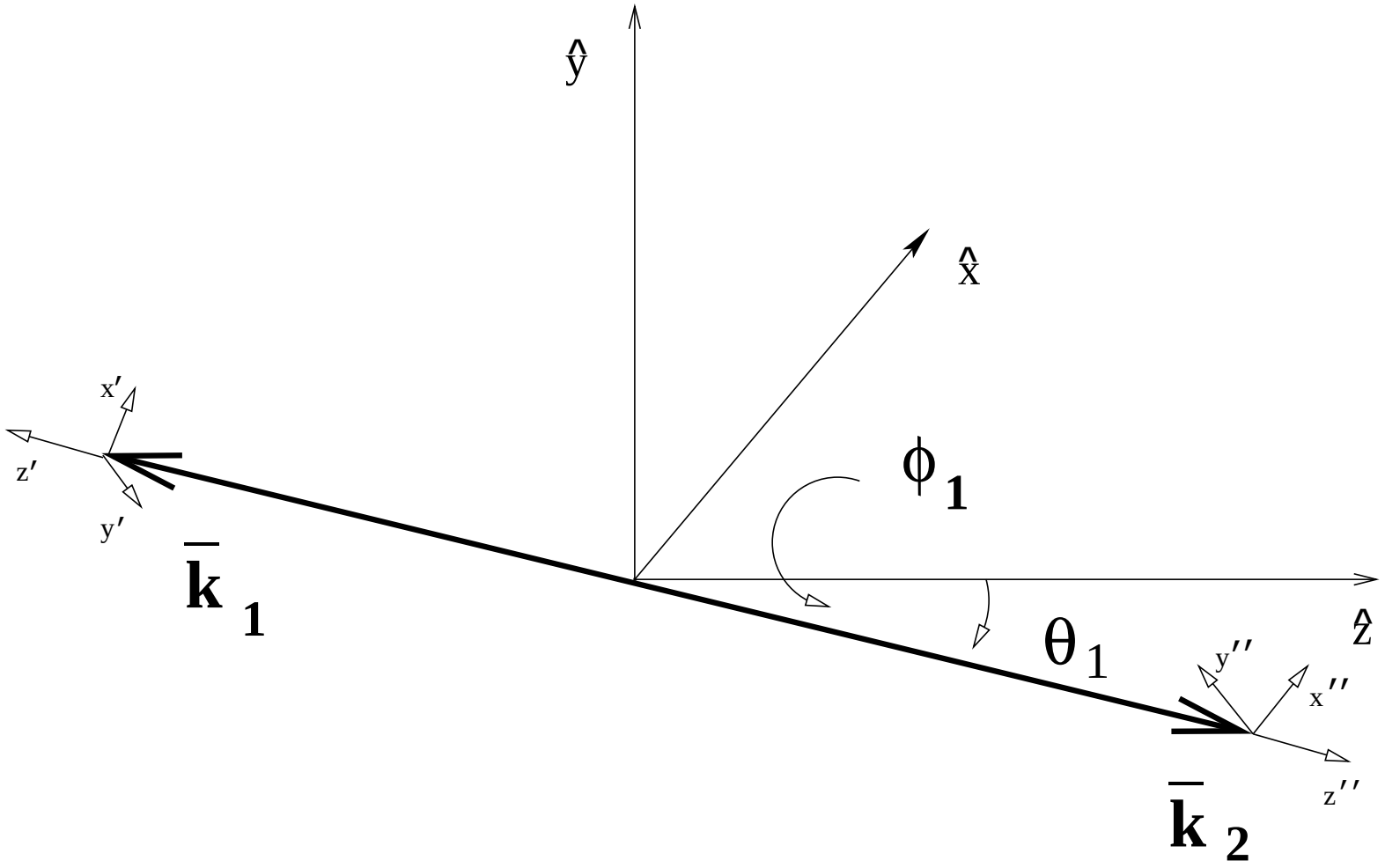

Figure 7: The angles θ_1, ϕ_1 defined in the rest-frame of P and used in parametrization of two-body phase-space.

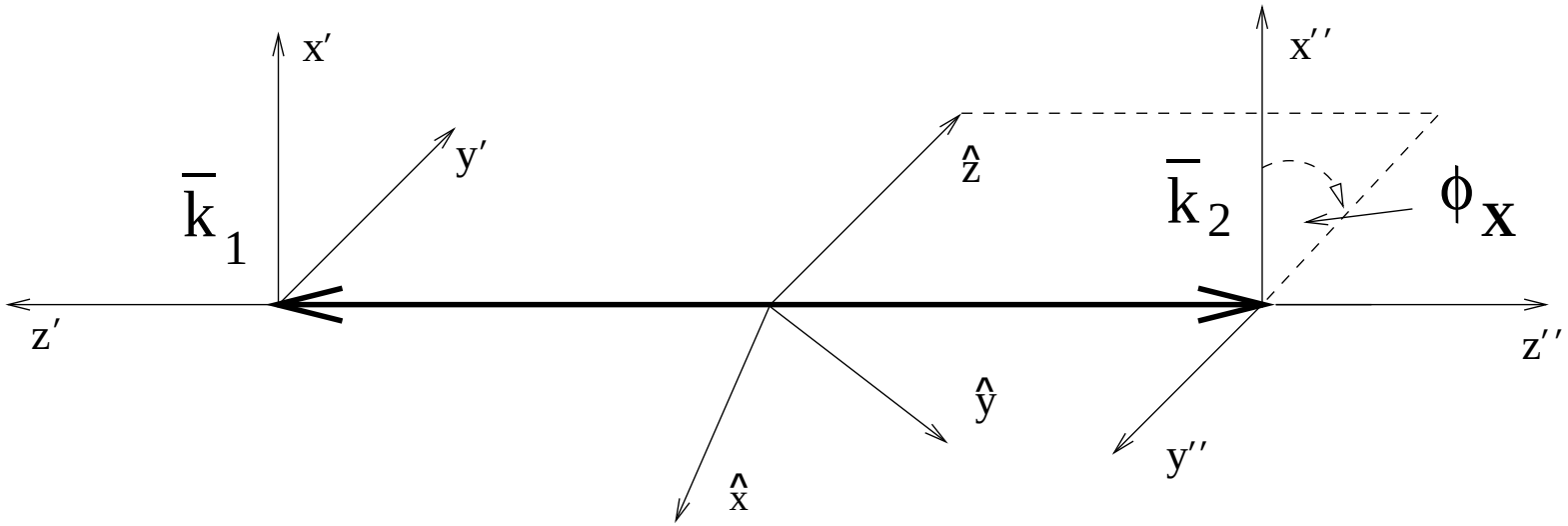

Figure 8: Angle ϕ_X is also defined in the rest-frame of P as an angle between (oriented) planes spanned on: (i) $\bar{k}_1$ and $\hat{z}$-axis of the P rest-frame system, and (ii) $\bar{k}_1$ and x''-axis of the $\bar{k}_2$ rest frame. It completes definition of the phase-space variables if internal orientation of $\bar{k}_1$ system is of interest. In fact, Euler angle ϕ_X is inherited from unspecified in details, parametrization of phase space used to describe possible future decay of $\bar{k}_2$ (or $\bar{k}_1$).

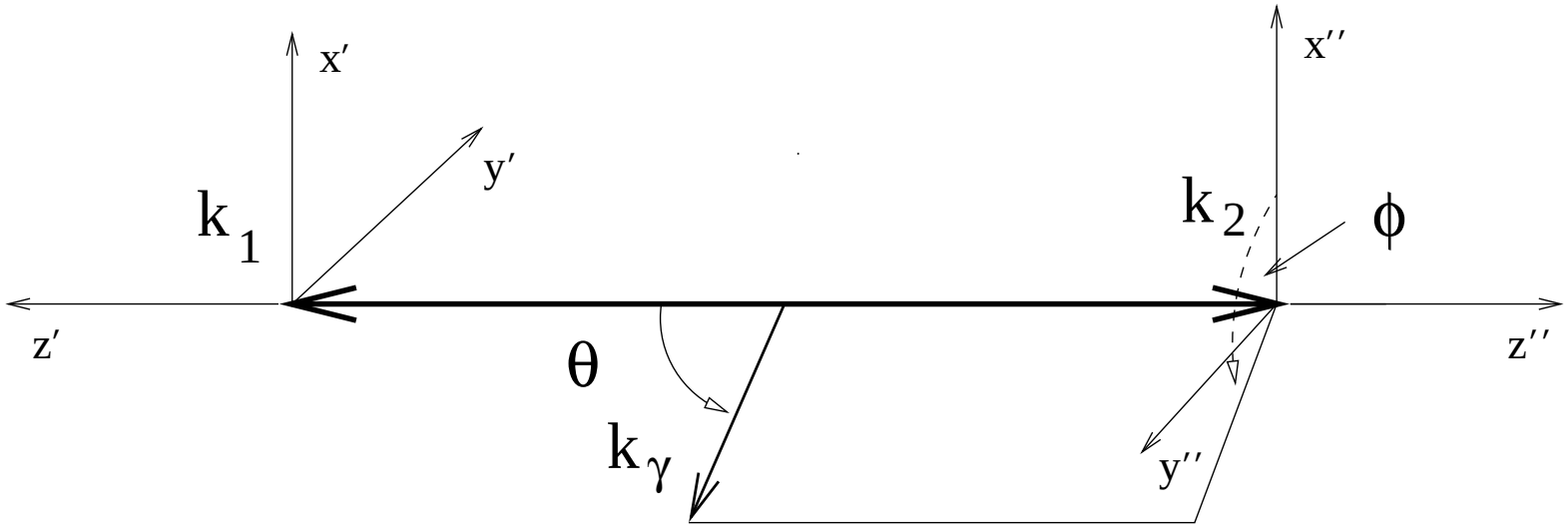

Figure 9: The angles θ, ϕ are used to construct the four-momentum of k_γ in the rest-frame of $k_1 + k_2$ pair (itself not yet oriented with respect to P rest-frame). To calculate energies of k_1, k_2 and photon, it is enough to know m_1, m_2, M and photon energy k_γ of the P rest-frame.

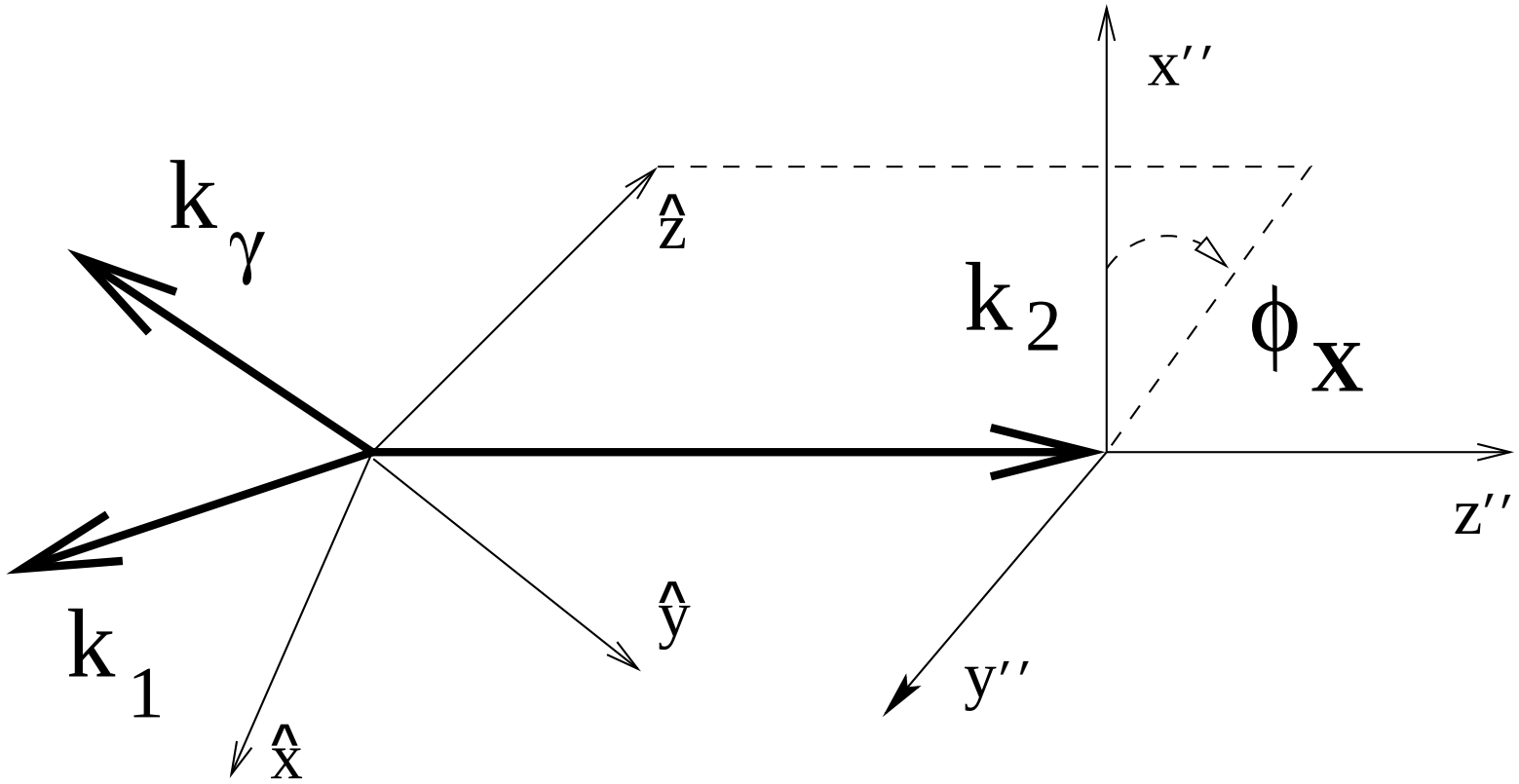

Figure 10: Use of angle ϕ_x in defining orientation of k_1, k_2 and photon in the rest-frame of P. At this step only the plane spanned on P frame axis $\hat{z}$ and k_2 is oriented with respect to $k_2 \times x''$ plane.

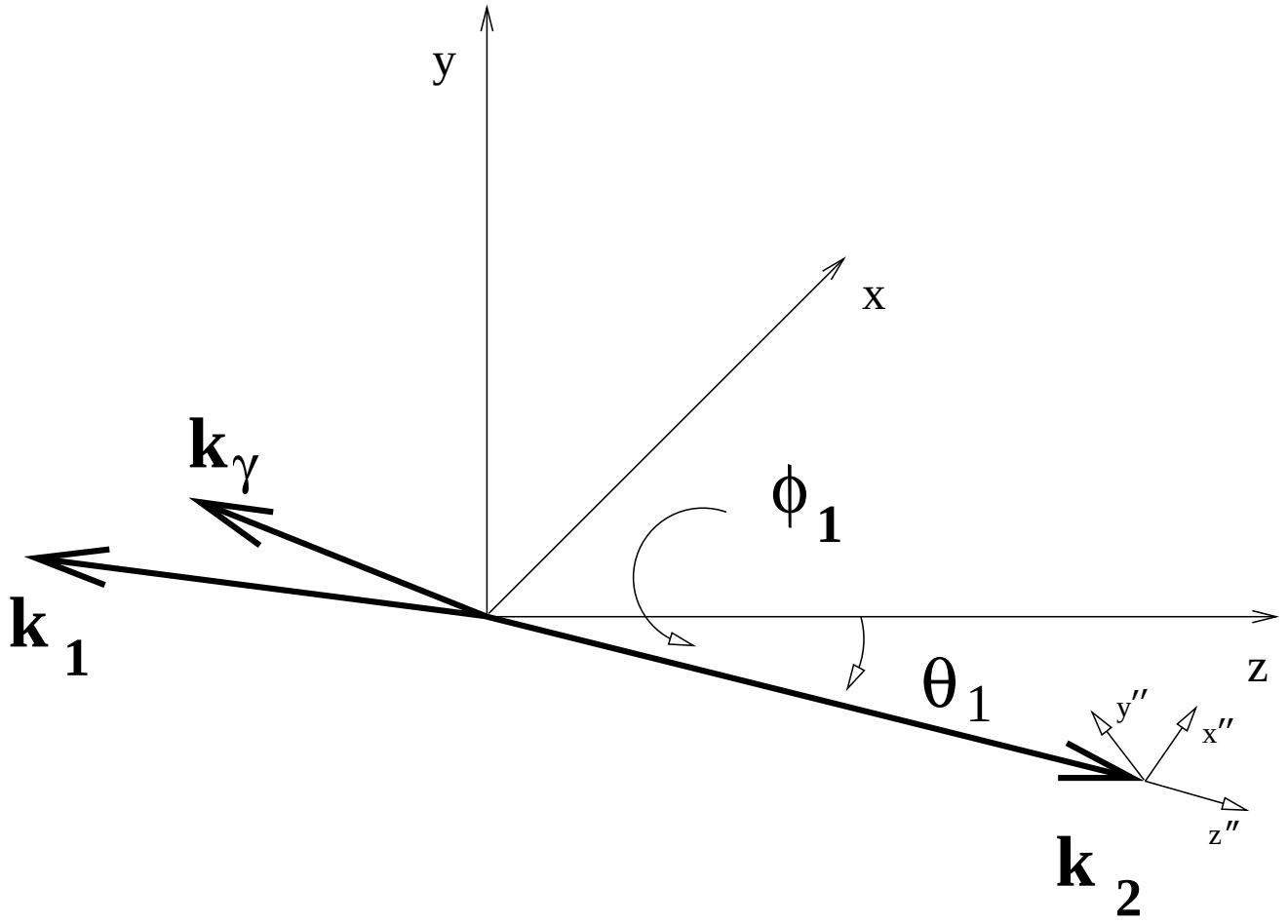

Figure 11: Final step in event construction. Angles θ_1, ϕ_1 are used. The final orientation of k_2 coincide with this of $\bar{k}_2$.